

MIRROR DESCENT ACTOR CRITIC VIA BOUNDED ADVANTAGE LEARNING

Ryo Iwaki

IBM Research - Tokyo

Ryo.Iwaki@ibm.com

ABSTRACT

Regularization is a core component of recent Reinforcement Learning (RL) algorithms. Mirror Descent Value Iteration (MDVI) uses both Kullback-Leibler divergence and entropy as regularizers in its value and policy updates. Despite its empirical success in discrete action domains and strong theoretical guarantees, the performance of a MDVI-based method does not surpass an entropy-only-regularized method in continuous action domains. In this study, we propose Mirror Descent Actor Critic (MDAC) as an actor-critic style instantiation of MDVI for continuous action domains, and show that its empirical performance is significantly boosted by bounding the actor’s log-density terms in the critic’s loss function, compared to a non-bounded naive instantiation. Further, we relate MDAC to Advantage Learning by recalling that the actor’s log-probability is equal to the regularized advantage function in tabular cases, and theoretically discuss when and why bounding the advantage terms is validated and beneficial. We also empirically explore a good choice for the bounding function, and show that MDAC performs better than strong non-regularized and entropy-only-regularized methods with an appropriate choice of the bounding function.

1 INTRODUCTION

Model-free reinforcement learning (RL) is a promising approach to obtain reasonable controllers in unknown environments. In particular, actor-critic (AC) methods are appealing because they can be naturally applied to continuous control domains. AC algorithms have been applied in a range of challenging domains including robot control (Smith et al., 2023), tokamak plasma control (Degraeve et al., 2022), and alignment of large language models (Stiennon et al., 2020).

Regularization is a core component of, not only such AC methods, but also value-based reinforcement learning algorithms (Peters et al., 2010; Azar et al., 2012; Schulman et al., 2015; 2017; Haarnoja et al., 2017; 2018a; Abdolmaleki et al., 2018). Kullback-Leibler (KL) divergence and entropy are two major regularizers that have been adopted to derive many successful algorithms. In particular, Mirror Descent Value Iteration (MDVI) uses both KL divergence and entropy as regularizers in its value and policy updates (Geist et al., 2019; Vieillard et al., 2020a) and enjoys strong theoretical guarantees (Vieillard et al., 2020a; Kozuno et al., 2022). However, despite its empirical success in discrete action domains (Vieillard et al., 2020b), the performance of a MDVI-based algorithm does not surpass an entropy-only-regularized method in continuous action domains (Vieillard et al., 2022).

In this study, we propose Mirror Descent Actor Critic (MDAC) as a model-free actor-critic instantiation of MDVI for continuous action domains, and show that its empirical performance is significantly boosted by bounding the actor’s log-density terms in the critic’s loss function, compared to a non-bounded naive instantiation. To understand the impact of bounding beyond just as an “implementation detail”, we relate MDAC to Advantage Learning (AL) (Baird, 1999; Bellemare et al., 2016) by recalling that the policy’s log-probability is equal to the regularized soft advantage function in tabular case, and theoretically discuss when and why bounding the advantage terms is validated and beneficial. Our analysis indicates that it is beneficial to bound the log-policy term of not only the current state-action pair but also the successor pair in the TD target signal.

Related Works. The key component of our actor-critic algorithm is to bound the log-policy terms in the critic loss, which can be also understood as bounding the regularized advantages. Munchausen RL clips the log-policy term for the current state-action pair, which serves as an augmented reward, as an implementation issue (Vieillard et al., 2020b). Our analysis further supports the empirical success of Munchausen algorithms. Zhang et al. (2022) extended AL by introducing a clipping strategy, which increases the action gap only when the action values of suboptimal actions exceed a certain threshold. Our bounding strategy is different from theirs in the way that the action gap is increased for all state-action pairs but with bounded amounts. Vieillard et al. (2022) proposed a sound parameterization of Q-function that uses log-policy. By construction, the regularized greedy step of MDVI can be performed exactly even in actor-critic settings with their parameterization. Our study is orthogonal to theirs since our approach modifies not the parameterization of the critic but its loss function.

MDVI and its variants are instances of mirror descent (MD) based RL. There are substantial research efforts in this direction (Wang et al., 2019; Vaswani et al., 2022; Kuba et al., 2022; Yang et al., 2022; Tomar et al., 2022; Lan, 2023; Alfano et al., 2023). The MD perspective enables to understand the existing algorithms in a unified view, analyze such methods with strong theoretical tools, and propose a novel and superior one. Further discussion on MD based methods are provided in Appendix A. This paper focuses on a specific choice of mirror, i.e. adopting KL divergence and entropy as regularizers, and provides a deeper understanding in this specific scope via a notion of *gap-increasing* operators.

It is well known that the log-policy terms in AC algorithms often cause instability, since the magnitude of log-policy terms grow large naturally in MDP, where a deterministic policy is optimal. Recent RL implementations handle this problem by bounding the range of the standard deviation for Gaussian policies (Achiam, 2018; Huang et al., 2022). Beyond such an implementation detail, Silver et al. (2014) proposed to use deterministic policy gradient, which is a foundation of the recent actor-critic algorithms such as TD3 (Fujimoto et al., 2018). Iwaki & Asada (2019) proposed an implicit iteration method to stably estimate the natural policy gradient (Kakade, 2001), which also can be viewed as a MD-based RL method (Thomas et al., 2013).

Contributions. Our contributions are summarized as follows: (1) we proposed MDAC, a model-free actor-critic instantiation of MDVI for continuous action domains, and showed that its empirical performance is significantly boosted by bounding the actor’s log-density terms in the critic’s loss function, compared to a non-bounded naive instantiation. (2) We theoretically analyzed the validity and the effectiveness of the bounding strategy by relating MDAC to AL with bounded advantage terms. To be specific, (2-1) we provided sufficient conditions under which the bounding strategy results in asymptotic convergence, which also suggests that Munchausen RL is convergent even when the ad-hoc clipping is employed, and (2-1) we showed that the bounding strategy reduces *inherent errors* of gap-increasing Bellman operators. (3) We empirically explored what types of bounding functions are effective. (4) We demonstrated that MDAC performs better than strong non-regularized and entropy-only-regularized baseline methods in simulated benchmarks.

2 PRELIMINARY

MDP and Approximate Value Iteration. A Markov Decision Process (MDP) is specified by a tuple $(\mathcal{S}, \mathcal{A}, P, R, \gamma)$, where \mathcal{S} is a state space, \mathcal{A} is an action space, P is a Markovian transition kernel, R is a reward function bounded by R_{\max} , and $\gamma \in (0, 1)$ is a discount factor. For $\tau \geq 0$, we write $V_{\max}^{\tau} = \frac{R_{\max} + \tau \log |\mathcal{A}|}{1 - \gamma}$ (assuming \mathcal{A} is finite) and $V_{\max} = V_{\max}^0$. We write $\mathbf{1} \in \mathbb{R}^{\mathcal{S} \times \mathcal{A}}$ the vector whose components are all equal to one. A policy π is a distribution over actions given a state. Let Π denote a set of Markovian policies. The state-action value function associated with a policy π is defined as $Q^{\pi}(s, a) = \mathbb{E}_{\pi} [\sum_{t=0}^{\infty} \gamma^t R(S_t, A_t) | S_0 = s, A_0 = a]$, where \mathbb{E}_{π} is the expectation over trajectories generated under π . An optimal policy satisfies $\pi^* \in \operatorname{argmax}_{\pi \in \Pi} Q^{\pi}$ with the understanding that operators are point-wise, and $Q^* = Q^{\pi^*}$. For $f_1, f_2 \in \mathbb{R}^{\mathcal{S} \times \mathcal{A}}$, we define a component-wise

dot product $\langle f_1, f_2 \rangle = (\sum_a f_1(s, a) f_2(s, a))_s \in \mathbb{R}^S$. Let P_π denote the stochastic kernel induced by π . For $Q \in \mathbb{R}^{S \times \mathcal{A}}$, let us define $P_\pi Q = (\sum_{s'} P(s'|s, a) \sum_{a'} \pi(a'|s') Q(s', a'))_{s, a} \in \mathbb{R}^{S \times \mathcal{A}}$. Furthermore, for $V \in \mathbb{R}^S$ let us define $PV = (\sum_{s'} P(s'|s, a) V(s'))_{s, a} \in \mathbb{R}^{S \times \mathcal{A}}$ and $P^\pi V = (\sum_a \pi(a|s) \sum_{s'} P(s'|s, a) V(s'))_s \in \mathbb{R}^S$. It holds that $P_\pi Q = P\langle \pi, Q \rangle$. The Bellman operator is defined as $\mathcal{T}_\pi Q = R + \gamma P_\pi Q$, whose unique fixed point is Q^π . The set of greedy policies w.r.t. $Q \in \mathbb{R}^{S \times \mathcal{A}}$ is written as $\mathcal{G}(Q) = \operatorname{argmax}_{\pi \in \Pi} \langle Q, \pi \rangle$. Approximate Value Iteration (AVI) (Bellman & Dreyfus, 1959) is a classical approach to estimate an optimal policy. Let $Q_0 \in \mathbb{R}^{S \times \mathcal{A}}$ be initialized as $\|Q_0\|_\infty \leq V_{\max}$ and $\epsilon_k \in \mathbb{R}^{S \times \mathcal{A}}$ represent approximation/estimation errors. Then, AVI can be written as the following abstract form:

$$\begin{cases} \pi_{k+1} \in \mathcal{G}(Q_k) \\ Q_{k+1} = \mathcal{T}_{\pi_{k+1}} Q_k + \epsilon_{k+1} \end{cases} .$$

Regularized MDP and MDVI. In this study, we consider the Mirror Descent Value Iteration (MDVI) scheme (Geist et al., 2019; Vieillard et al., 2020a). Let us define the entropy $\mathcal{H}(\pi) = -\langle \pi, \log \pi \rangle \in \mathbb{R}^S$ and the KL divergence $D_{\text{KL}}(\pi_1 \| \pi_2) = \langle \pi_1, \log \pi_1 - \log \pi_2 \rangle \in \mathbb{R}_{\geq 0}^S$. For $Q \in \mathbb{R}^{S \times \mathcal{A}}$ and a reference policy $\mu \in \Pi$, we define the regularized greedy policy as $\mathcal{G}_\mu^{\lambda, \tau}(Q) = \operatorname{argmax}_{\pi \in \Pi} (\langle \pi, Q \rangle + \tau \mathcal{H}(\pi) - \lambda D_{\text{KL}}(\pi \| \mu))$. We write $\mathcal{G}^{0, \tau}$ for $\lambda = 0$ and $\mathcal{G}^{0, 0}(Q) = \mathcal{G}(Q)$. We define the soft state value function $V(s) \in \mathbb{R}^S$ as $V(s) = \langle \pi, Q \rangle + \tau \mathcal{H}(\pi) - \lambda D_{\text{KL}}(\pi \| \mu)$, where $\pi = \mathcal{G}_\mu^{\lambda, \tau}(Q)$. Furthermore, we define the regularized Bellman operator as $\mathcal{T}_{\pi|\mu}^{\lambda, \tau} Q = R + \gamma P (\langle \pi, Q \rangle + \tau \mathcal{H}(\pi) - \lambda D_{\text{KL}}(\pi \| \mu))$. Given these notations, MDVI scheme is defined as

$$\begin{cases} \pi_{k+1} = \mathcal{G}_{\pi_k}^{\lambda, \tau}(Q_k) \\ Q_{k+1} = \mathcal{T}_{\pi_{k+1}|\pi_k}^{\lambda, \tau} Q_k + \epsilon_{k+1} \end{cases} , \quad (1)$$

where π_0 is initialized as the uniform policy.

Vieillard et al. (2020b) proposed a reparameterization $\Psi_k = Q_k + \beta \alpha \log \pi_k$. Then, defining $\alpha = \tau + \lambda$ and $\beta = \lambda / (\tau + \lambda)$, the recursion (1) can be rewritten as

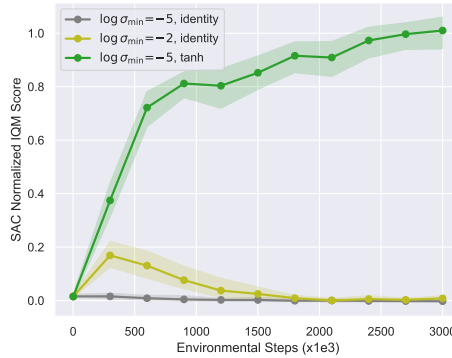
$$\begin{cases} \pi_{k+1} = \mathcal{G}^{0, \alpha}(\Psi_k) \\ \Psi_{k+1} = R + \gamma P \langle \pi_{k+1}, \Psi_k - \alpha \log \pi_{k+1} \rangle + \beta \alpha \log \pi_{k+1} + \epsilon_{k+1} \end{cases} . \quad (2)$$

We refer (2) as Munchausen Value Iteration (M-VI). In the recursion (2), KL regularization is implicitly applied through Ψ_k and there is no need to store π_k for explicit computation of the KL term. Notice that the regularized greedy policy $\pi_{k+1} = \mathcal{G}^{0, \alpha}(\Psi_k)$ can be obtained analytically in discrete action spaces as $(\mathcal{G}^{0, \alpha}(\Psi_k))(s, a) = \frac{\exp \Psi_k(s, a) / \alpha}{\langle \mathbf{1}, \exp \Psi_k(s, a) / \alpha \rangle} =: (\text{sm}_\alpha(\Psi_k))(s, a)$.

3 MIRROR DESCENT ACTOR CRITIC WITH BOUNDED BONUS TERMS

In this section, we introduce a model-free actor-critic instantiation of MDVI for continuous action domains, and show that a naive implementation results in poor performance. Then, we demonstrate that its performance is improved significantly by a simple modification to its loss function.

Now we derive Mirror Descent Actor Critic (MDAC). Let π_θ be a tractable stochastic policy such as a Gaussian with a parameter θ . Let Q_ψ be a value function with a parameter ψ . The functions π_θ and Q_ψ approximate π_k and Ψ_k in the recursion (2), respectively. Further, let $\bar{\psi}$ be a target parameter that is updated slowly, that is, $\bar{\psi} \leftarrow (1 - \kappa) \bar{\psi} + \kappa \psi$ with $\kappa \in (0, 1)$. Let \mathcal{D} be a replay buffer that stores past experiences $\{(s, a, r, s')\}$. We can derive model-free and off-policy losses from the recursion (2) for the actor π_θ and the critic Q_ψ by (i) letting the parameterized policy π_θ be represent the information projection of π_k in terms of the KL divergence, and (ii) approximating the expectations using the transition samples drawn

Figure 1: Effect of bounding $\alpha \log \pi_\theta$ terms.

from \mathcal{D} :

$$L^Q(\psi) = \mathbb{E}_{\substack{(s,a,r;s') \sim \mathcal{D}, \\ a' \sim \pi_\theta(\cdot|s')}} \left[(y - Q_\psi(s, a))^2 \right], \quad (3)$$

$$y = r + \beta \alpha \log \pi_\theta(a|s) + \gamma (Q_{\bar{\psi}}(s', a') - \alpha \log \pi_\theta(a'|s')), \quad (4)$$

$$L^\pi(\theta) = \mathbb{E}_{\substack{s \sim \mathcal{D}, \\ a \sim \pi_\theta(\cdot|s)}} \left[D_{\text{KL}}(\pi_\theta(a|s) \parallel \text{sm}_\alpha(Q_\psi)(s, a)) \right] = \mathbb{E}_{\substack{s \sim \mathcal{D}, \\ a \sim \pi_\theta(\cdot|s)}} \left[\alpha \log \pi_\theta(a|s) - Q_\psi(s, a) \right]. \quad (5)$$

Though π_θ can be any tractable distribution, we choose commonly used Gaussian policy in this paper. We lower-bound its standard deviation by a common hyperparameter $\log \sigma_{\min}$, which is typically fixed to $\log \sigma_{\min} = -20$ (Huang et al., 2022) or $\log \sigma_{\min} = -5$ (Achiam, 2018). Although there are two hyperparameters α and β originated from KL and entropy regularization, these hyperparameters need not to be tuned manually. We fixed $\beta = 1 - (1 - \gamma)^2$ as the theory of MDVI suggests (Kozuno et al., 2022). For α , we perform an optimization process similar to SAC (Haarnoja et al., 2018b). Noticing that the strength of the entropy regularization is governed by $\tau = (1 - \beta)\alpha$, we optimize the following loss in terms of α with $\bar{\mathcal{H}} = -\dim(\mathcal{A})$:

$$L(\alpha) = (1 - \beta)\alpha \mathbb{E}_{\substack{s \sim \mathcal{D}, \\ a \sim \pi_\theta(\cdot|s)}} \left[-\log \pi_\theta(a|s) - \bar{\mathcal{H}} \right]. \quad (6)$$

The reader may notice that (3) and (5) are nothing more than SAC losses (Haarnoja et al., 2018a;b) with the Munchausen augmented reward (Veillard et al., 2020b), and expect that optimizing these losses results in good performance. However, a naive implementation of these losses leads to poor performance. The gray learning curve in Figure 1 is an aggregated learning result for 6 Mujoco environments with $\log \sigma_{\min} = -5$ ¹. The left column of Figure 2 compares the quantities in the loss functions for the initial learning phase in HalfCheetah-v4. Clearly, the magnitude of $\log \pi_\theta$ terms gets much larger than the reward quickly. We hypothesized that the poor performance of the naive implementation is due to this scale difference; the information of the reward is erased by the bonus terms. This explosion is more severe in the Munchausen bonus $\beta \alpha \log \pi_\theta(a|s)$ than the entropy bonus $\alpha \log \pi_\theta(a'|s')$, because while a' is an *on-policy* sample from the current actor π_θ , a is an old *off-policy* sample from the replay buffer \mathcal{D} . Careful readers may wonder if the larger $\log \sigma_{\min}$ resolves this issue. The yellow learning curve in Figure 1 is the learning result for $\log \sigma_{\min} = -2$, which still fails to learn. The middle column of Figure 2 shows that the bonus terms are still divergent, and it is caused by the exploding behavior of α . A naive update of α using the loss (6) and SGD with a step-size $\rho > 0$ is expressed as

$$\alpha \leftarrow \alpha + \frac{\rho(1 - \beta)}{N} \sum_{n=1}^N (\log \pi_\theta(a_n|s_n) - \dim(\mathcal{A})),$$

¹Details on the setup and the metrics can be found in Section 5, and Figure 12 in Appendix C.2 shows the per-environment results.

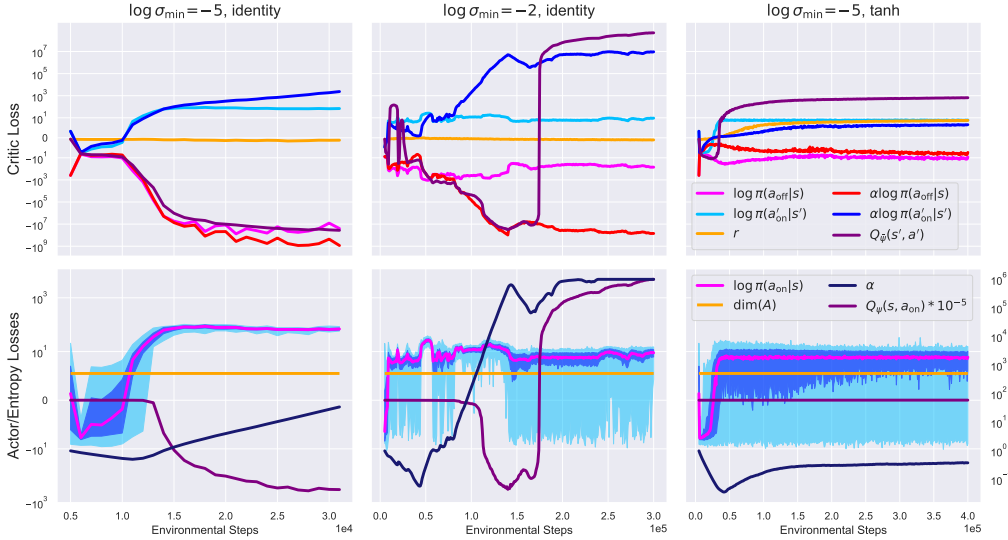


Figure 2: Scale comparison of the quantities in loss functions. The means of the quantities over the multiple sampled minibatches are plotted. Left: $\log \sigma_{\min} = -5$, Middle: $\log \sigma_{\min} = -2$, Right: $\log \sigma_{\min} = -5$ with bounding by tanh. Top: comparison in critic loss (3), Bottom: comparison in actor and entropy losses (5) and (6). α is indicated by the right y-axis. Blue shaded areas indicate standard deviations. Light blue shaded areas indicate minimum and maximum values.

where N is a mini-batch size, s_n is a sampled state in a mini-batch and $a_n \sim \pi_\theta(\cdot|s_n)$. This expression indicates that, if the averages of $\log \pi_\theta(a|s)$ over the sampled mini-batches are bigger than $\dim(\mathcal{A})$ over the iterations, α keeps growing. The bottom row of left and middle plots in Figure 2 indicates that this phenomenon is indeed happening. We argue that, an unstable behavior of a single component ruins the other learning components through the actor-critic structure. Through the loss (5), $\log \pi_\theta$ concentrates to high value, which makes α grow. Then, $\alpha \log \pi_\theta$ terms explode and hinder Q_ψ , and $\log \pi_\theta$ stays ruined.

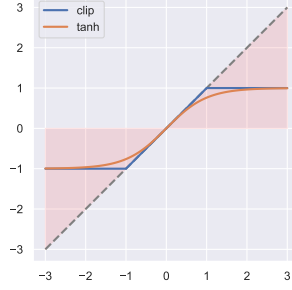
We found that “bounding” $\alpha \log \pi_\theta$ terms improves the performance significantly. To be precise, by replacing the target y in the critic’s loss (3) with the following, the agent succeeds to reach reasonable performance (the green learning curve in Figure 1; $\log \sigma_{\min} = -5$ is used):

$$y = r + \beta \tanh(\alpha \log \pi_\theta(a|s)) + \gamma (Q_{\bar{\psi}}(s', a') - \tanh(\alpha \log \pi_\theta(a'|s'))). \quad (7)$$

The right column of Figure 2 shows that with this target (7), $\alpha \log \pi_\theta$ terms do not explode since $\log \pi_\theta$ does not concentrate to high value and α does not grow, and Q_ψ is not ruined. In the next section, we analyze what happens under the hood by theoretically investigating the effect of bounding $\alpha \log \pi_\theta$ terms. We argue that bounding $\alpha \log \pi_\theta$ terms is not just an ad-hoc implementation issue, but it changes the property of the underlying Bellman operator. We quantify the amount of ruin caused by $\alpha \log \pi_\theta$ terms, and show how this negative effect is mitigated by the bounding.

4 ANALYSIS

In this section, we theoretically investigate the properties of the log-policy-bounded target (7) in tabular settings. Rather than analyzing a specific choice of bounding, e.g. $\tanh(x)$, we characterize the conditions for bounding functions that are validated and effective. For the sake of analysis, we provide an abstract dynamic programming scheme of the log-policy-bounded target (7) and relate it to Advantage Learning (Baird, 1999; Bellemare et al., 2016) in Section 4.1. In Section 4.2, we show that carefully chosen bounding function ensures asymptotically convergence. In Section 4.3, we show that such bounding is indeed beneficial in terms of inherent error reduction property. All the proofs will be found in Appendix B.

Figure 3: Examples of f, g .

4.1 BOUNDED ADVANTAGE LEARNING

Let f and g be non-decreasing functions over \mathbb{R} such that, for both $h \in \{f, g\}$, (i) $h(x) > 0$ for $x > 0$, $h(x) < 0$ for $x < 0$ and $h(0) = 0$, (ii) $x - h(x) \geq 0$ for $x \geq 0$ and $x - h(x) \leq 0$ for $x \leq 0$, and (iii) their codomains are connected subsets of $[-c_h, c_h]$. The functions $\tanh(x)$ and $\text{clip}(x, -1, 1)$ satisfy these conditions. We understand that the identity map I also satisfies these conditions with $c_h \rightarrow \infty$. Roughly speaking, we require the functions f and g to lie in the shaded area in Figure 3. Then, the loss (3), (5) and (7) can be seen as an instantiation of the following abstract VI scheme:

$$\begin{cases} \pi_{k+1} = \mathcal{G}^{0,\alpha}(\Psi_k) \\ \Psi_{k+1} = R + \beta f(\alpha \log \pi_{k+1}) + \gamma P \langle \pi_{k+1}, \Psi_k - g(\alpha \log \pi_{k+1}) \rangle + \epsilon_{k+1} \end{cases} \quad (8)$$

Notice that Munchausen-DQN and its variants are instantiations of this scheme, since their implementations clip the Munchausen bonus term by $f(x) = [x]_{l_0}^0$ with $l_0 = -1$ typically, while $g = I$. Furthermore, if we choose $f = g \equiv 0$, (8) reduces to Expected Sarsa (van Seijen et al., 2009).

Now, from the basic property of regularized MDPs, the soft state value function $V \in \mathbb{R}^{\mathcal{S}}$ satisfies $V = \alpha \log \langle \mu^\beta, \exp \frac{Q}{\alpha} \rangle = \alpha \log \langle \mathbf{1}, \exp \frac{\Psi}{\alpha} \rangle$, where $\Psi = Q + \beta \alpha \log \mu$. We write $\mathbb{L}^\alpha \Psi = \alpha \log \langle \mathbf{1}, \exp \frac{\Psi}{\alpha} \rangle$ for convention. The basic properties of \mathbb{L}^α are summarized in Appendix B.1. In the limit $\alpha \rightarrow 0$, it holds that $V(s) = \max_{a \in \mathcal{A}} \Psi(s, a)$. Furthermore, for a policy $\pi = \mathcal{G}^{0,\alpha}(\Psi)$, $\alpha \log \pi$ equals to the soft advantage function $A \in \mathbb{R}^{\mathcal{S} \times \mathcal{A}}$:

$$\alpha \log \pi = \alpha \log \frac{\exp \frac{\Psi}{\alpha}}{\langle \mathbf{1}, \exp \frac{\Psi}{\alpha} \rangle} = \alpha \log \exp \left(\frac{\Psi - V}{\alpha} \right) = \Psi - V =: A,$$

thus we have that $\alpha \log \pi_{k+1} = A_k$. Therefore, as discussed by Vieillard et al. (2020a), the recursion (2) is written as a soft variant of Advantage Learning (AL):

$$\begin{aligned} \Psi_{k+1} &= R + \beta A_k + \gamma P \langle \pi_{k+1}, \Psi_k - A_k \rangle + \epsilon_{k+1} \\ &= R + \gamma P V_k - \beta (V_k - \Psi_k) + \epsilon_{k+1}. \end{aligned}$$

Given these observations, we introduce a *bounded gap-increasing Bellman operator* $\mathcal{T}_{\pi_{k+1}}^{fg}$:

$$\mathcal{T}_{\pi_{k+1}}^{fg} \Psi_k = R + \beta f(A_k) + \gamma P \langle \pi_{k+1}, \Psi_k - g(A_k) \rangle. \quad (9)$$

Then, the DP scheme (8) is equivalent to the following *Bounded Advantage Learning* (BAL):

$$\begin{cases} \pi_{k+1} = \mathcal{G}^{0,\alpha}(\Psi_k) \\ \Psi_{k+1} = \mathcal{T}_{\pi_{k+1}}^{fg} \Psi_k + \epsilon_{k+1} \end{cases} \quad (10)$$

By construction, the operator $\mathcal{T}_{\pi_{k+1}}^{fg}$ pushes-down the value of actions. To be precise, since $\max_{a \in \mathcal{A}} \Psi(s, a) \leq (\mathbb{L}^\alpha \Psi)(s)$, the soft advantage A_k is always non-positive. Thus, the reparameterized action value Ψ_k is decreased by adding the term $\beta f(A_k)$. The decrement is smallest at the optimal action $\arg \max_a \Psi_k(s, a)$. Therefore, the operator $\mathcal{T}_{\pi_{k+1}}^{fg}$ increases

the action gaps with bounded magnitude dependent on f . The increased action gap is advantageous in the presence of approximation or estimation errors ϵ_k (Farahmand, 2011; Bellemare et al., 2016). In addition, as the term $-\gamma P \langle \pi_{k+1}, g(A_k) \rangle$ in Eq. (9) indicates, the entropy bonus for the successor state action pair $(s', a') \sim P_\pi(\cdot|s, a)$ is decreased by g .

We remark that BAL preserves the original mirror descent structure of MDVI (1). Noticing that $Q_k = \Psi_k - \beta \alpha \log \pi_k$, $(1 - \beta)\alpha = \tau$ and $\beta\alpha = \lambda$, and following some steps similar to the derivation of Munchausen RL in Appendix A.2 of (Vieillard et al., 2020b), the bounded gap-increasing operator (9) can be rewritten in terms of Q as

$$\mathcal{T}_{\pi_{k+1}|\pi_k}^{fg} \Psi_k = \mathcal{T}_{\pi_{k+1}|\pi_k}^{\lambda, \tau} Q_k - \beta (A_k - f(A_k)) + \gamma P \langle \pi_{k+1}, A_k - g(A_k) \rangle.$$

Therefore, BAL still aligns the the original mirror descent structure of MDVI, but with additional modifications to the Bellman backup term.

4.2 CONVERGENCE OF BAL

First, we investigate the *asymptotic* convergence property of BAL scheme. Since gap-increasing operators are *not contraction maps* in general, we need an argument similar to the analysis provided by Bellemare et al. (2016). Indeed, for the case where $\alpha \rightarrow 0$ while keeping β constant, which corresponds to KL-only regularization and hard gap-increasing, their asymptotic result directly applies and it is guaranteed that BAL is *optimality-preserving* (please see Appendix B.2). On the other hand, however, we need tailored analyses for the case $\alpha > 0$. The following theorem characterizes the possibly biased convergence of soft gap-increasing operators under KL-entropy regularization.

Theorem 1. *Let $\Psi \in \mathbb{R}^{S \times \mathcal{A}}$, $V = \mathbb{L}^\alpha \Psi$, $\mathcal{T}^\alpha \Psi = R + \gamma P \mathbb{L}^\alpha \Psi$ and \mathcal{T}' be an operator with the properties that $\mathcal{T}' \Psi \leq \mathcal{T}^\alpha \Psi$ and $\mathcal{T}' \Psi \geq \mathcal{T}^\alpha \Psi - \beta (V - \Psi)$. Consider the sequence $\Psi_{k+1} := \mathcal{T}' \Psi_k$ with $\Psi_0 \in \mathbb{R}^{S \times \mathcal{A}}$, and let $V_k = \mathbb{L}^\alpha \Psi_k$. Further, with an abuse of notation, we write $V_\tau^* \in \mathbb{R}^S$ as the unique fixed point of the operator $\mathcal{T}^\tau V = \mathbb{L}^\tau (R + \gamma P V)$. Then, the sequence $(V_k)_{k \in \mathbb{N}}$ converges, and the limit $\tilde{V} = \lim_{k \rightarrow \infty} V_k$ satisfies $V_\tau^* \leq \tilde{V} \leq V_\alpha^*$. Furthermore, $\limsup_{k \rightarrow \infty} \Psi_k \leq Q_\alpha^*$ and $\liminf_{k \rightarrow \infty} \Psi_k \geq \frac{1}{1-\beta} (\tilde{Q} - \beta \tilde{V})$, where $\tilde{Q} = R + \gamma P \tilde{V}$.*

Since $\mathcal{T}^\alpha \Psi_k \geq \mathcal{T}_{\pi_{k+1}}^{fI} \Psi_k = \mathcal{T}^\alpha \Psi_k + \beta f(A_k) \geq \mathcal{T}^\alpha \Psi_k + \beta A_k$, from Theorem 1 we can assure that BAL is convergent and Ψ_k remains in a bounded range if $g = I$, even though $\tilde{V} \neq V_\tau^*$ in general. Furthermore, this result suggests that *Munchausen RL is convergent even when the ad-hoc clipping is employed*. However, Theorem 1 does not support the convergence for $g \neq I$, even though $g \neq I$ is empirically beneficial as seen in Section 3. The following Proposition 1 offers a sufficient condition for the asymptotic convergence when $g \neq I$, and characterizes the limiting behavior of BAL.

Proposition 1. *Consider the sequence $\Psi_{k+1} := \mathcal{T}_{\pi_{k+1}}^{fg} \Psi_k$ produced by the BAL operator (9) with $\Psi_0 \in \mathbb{R}^{S \times \mathcal{A}}$, and let $V_k = \mathbb{L}^\alpha \Psi_k$. Assume that for all $k \in \mathbb{N}$ it holds that*

$$\lambda D_{k+1} - \gamma P^{\pi_{k+1}} (\alpha \mathcal{H}(\pi_{k+1}) + \langle \pi_{k+1}, g(A_k) \rangle) \geq 0, \quad (11)$$

where $D_{k+1} = D_{\text{KL}}(\pi_{k+1} \|\pi_k)$. Then, the sequence $(V_k)_{k \in \mathbb{N}}$ converges, and the limit $\tilde{V} = \lim_{k \rightarrow \infty} V_k$ satisfies $V_\alpha^* - \frac{1}{1-\gamma} (\beta c_f + \gamma \alpha \log |\mathcal{A}|) \leq \tilde{V} \leq V_\alpha^*$. Furthermore, $\limsup_{k \rightarrow \infty} \Psi_k \leq Q_\alpha^*$ and $\liminf_{k \rightarrow \infty} \Psi_k \geq \tilde{Q} - (\beta c_f + \gamma \alpha \log |\mathcal{A}|)$, where $\tilde{Q} = R + \gamma P \tilde{V}$.

We remark that the lower bound of \tilde{V} is reasonable. Since $V_{\max}^\alpha = V_{\max} + \frac{\alpha \log |\mathcal{A}|}{1-\gamma}$, the magnitude of the lower bound roughly matches the un-regularized value, which appears because g decreases the entropy bonus in the Bellman backup. One way to satisfy (11) for all $k \in \mathbb{N}$ is to use an adaptive strategy to determine g . Since π_{k+1} is obtained *before* the update $\Psi_{k+1} = \mathcal{T}_{\pi_{k+1}}^{fg} \Psi_k$ in BAL scheme (10), it is possible that we first compute $D_{\text{KL}}(\pi_{k+1} \|\pi_k)$ and $\mathcal{H}(\pi_{k+1})$, and then adaptively find g that satisfies (11), with additional computational efforts. In the following, however, we provide an error propagation analysis and argue that a fixed $g \neq I$ is indeed beneficial.

4.3 BOUNDING DECREASES THE INHERENT ERRORS

Theorem 1 indicates that BAL is convergent but possibly biased even when $g = I$. However, we can still upper-bound the error between the optimal entropy-regularized state value V_τ^* , which is the unique fixed point of the operator $\mathcal{T}^\tau V = \mathbb{L}^\tau(R + \gamma PV)$, and the entropy-regularized state value $V_\tau^{\pi_k}$ for the sequence of the policies $(\pi_k)_{k \in \mathbb{N}}$ generated by BAL. Theorem 2 below, which generalizes Theorem 1 by Zhang et al. (2022) to KL-entropy-regularized settings with the bounding functions f and g , provides such a bound and highlights the advantage of BAL for both $f \neq I$ and $g \neq I$.

Theorem 2. *Let $(\pi_k)_{k \in \mathbb{N}}$ be a sequence of the policies obtained by BAL. Defining $\Delta_k^{fg} = \langle \pi^*, \beta(A_\tau^* - f(A_{k-1})) - \gamma P \langle \pi_k, A_{k-1} - g(A_{k-1}) \rangle \rangle$, it holds that:*

$$\|V_\tau^* - V_\tau^{\pi_{K+1}}\|_\infty \leq \frac{2\gamma}{1-\gamma} \left[2\gamma^{K-1} V_{\max}^\tau + \sum_{k=1}^{K-1} \gamma^{K-k-1} \|\Delta_k^{fg}\|_\infty \right]. \quad (12)$$

Since the suboptimality of BAL is characterized by Theorem 2, we can discuss its convergence property as in previous researches (Kozuno et al., 2019; Vieillard et al., 2020a). The bound (12) resembles the standard suboptimality bounds in the literature (Munos, 2005; 2007; Antos et al., 2008; Farahmand et al., 2010), which consists of the horizon term $2\gamma/(1-\gamma)$, initialization error $2\gamma^{K-1}V_{\max}^\tau$ that goes to zero as $K \rightarrow \infty$, and the accumulated error term. However, our error terms do not represent the Bellman backup errors, but capture *the misspecifications of the optimal policy* as we discuss later. We note that, the error term Δ_k^{fg} does not contain the error ϵ_k , because we simply omitted it in our analysis as done by Zhang et al. (2022). Our interest here is *not* in the effect of the approximation/estimation error ϵ_k , but in the effect of *the ruin caused by the soft advantage* $A_k = \alpha \log \pi_{k+1}$, that is, the error inherent to the soft-gap-increasing nature of M-VI and BAL in model-based tabular settings without any approximation. In the following, we consider a decomposition of the error $\Delta_k^{fg} = \Delta_k^{Xf} + \Delta_k^{Hg}$ and argue that (1) the cross term $\Delta_k^{Xf} = -\beta \langle \pi^*, f(A_{k-1}) \rangle$ has major effect on the sub-optimality and is *always* decreased by $f \neq I$, and (2) the entropy terms $\Delta_k^{Hg} = \langle \pi^*, \beta A_\tau^* - \gamma P \langle \pi_k, A_{k-1} - g(A_{k-1}) \rangle \rangle$ are decreased by $g \neq I$, although which is *not always* true.

To ease the exposition, first let us consider the case $\alpha \rightarrow 0$ while keeping $\beta > 0$ constant, which corresponds to KL-only regularization. Then, noticing that we have $\mathcal{G}^{0,0}(\Psi) = \mathcal{G}(\Psi)$, $\mathbb{L}^\alpha \Psi(s) \rightarrow \max_{b \in \mathcal{A}} \Psi(s, b)$ and $g(0)=0$, it follows that the entropy terms are equal to zero: $\langle \pi^*, A^* \rangle = \langle \pi_{k+1}, A_k \rangle = \langle \pi_{k+1}, g(A_k) \rangle = 0$. Thus, Δ_k^{fg} reduces to $\Delta_k^{Xf} = -\beta \langle \pi^*, f(A_{k-1}) \rangle$ and $\Delta_k^{Xf}(s) = -\beta f(\Psi_{k-1}(s, \pi^*(s)) - \Psi_{k-1}(s, \pi_k(s)))$. Therefore, Δ_k represents *the error incurred by the misspecification of the optimal policy*. For AL, the error is $\Delta_k^{XI}(s) = \beta(\Psi_{k-1}(s, \pi_k(s)) - \Psi_{k-1}(s, \pi^*(s)))$. Since both AL and BAL are optimality-preserving for $\alpha \rightarrow 0$, we have $\|\Delta_k^{XI}\|_\infty \rightarrow 0$ and $\|\Delta_k^{Xf}\|_\infty \rightarrow 0$ as $k \rightarrow \infty$. However, their convergence speed is governed by the magnitude of $\|\Delta_k^{XI}\|_\infty$ and $\|\Delta_k^{Xf}\|_\infty$ at finite k , respectively. We remark that for all k it holds that $|\Delta_k^{Xf}| \leq |\Delta_k^{XI}|$ point-wise. Indeed, from the non-positivity of A_k and the requirement to f , we always have $A_k = I(A_k) \leq f(A_k)$ point-wise and then $-\beta I(A_k(s, a)) \geq -\beta f(A_k(s, a))$ for all (s, a) and k , both sides of which are non-negative. Thus, we have $\langle \pi^*, -\beta f(A_{k-1}) \rangle \leq \langle \pi^*, -\beta I(A_{k-1}) \rangle$ point-wise and then $|\Delta_k^{Xf}| \leq |\Delta_k^{XI}|$. Further, we have $\|\Delta_k^{XI}\|_\infty \leq \frac{2R_{\max}}{1-\gamma}$ for AL while $\|\Delta_k^{Xf}\|_\infty \leq c_f$ for BAL. Therefore, BAL has better convergence property than AL by a factor of the horizon $1/(1-\gamma)$ when Ψ_k is far from optimal.

For the case $\alpha > 0$, $\|\Delta_k^{fg}\|_\infty \rightarrow 0$ does not hold in general. Further, the entropy terms are no longer equal to zero. However, the cross term, which is an order of $1/(1-\gamma)$, is much larger unless the action space is extremely large since the entropy is an order of $\log |\mathcal{A}|$ at most, and is always decreased by $f \neq I$. Furthermore, we can expect that $g \neq I$ decreases the error Δ_k^{Hg} , though it does *not always* true. If $g \neq I$, the entropy terms reduce to $\Delta_k^{HI} = \langle \pi^*, \beta A^* \rangle$. Since A_{k-1} is non-positive, we have $A_{k-1} - g(A_{k-1}) \leq 0$ from the requirements to g . Since the stochastic matrix P is non-negative, we have $P \langle \pi_k, A_{k-1} - g(A_{k-1}) \rangle \leq 0$, where the l.h.s. represents the decreased negative entropy of the successor state and its absolute

value is again an order of $\log|\mathcal{A}|$ at most. Since $A^* \leq 0$ also, whose absolute value is an order of $1/(1-\gamma)$, it holds that $\beta A^* \leq \beta A^* - \gamma P \langle \pi_k, A_{k-1} - g(A_{k-1}) \rangle$ and thus $\Delta_k^{\mathcal{H}I} = \langle \pi^*, \beta A^* \rangle \leq \langle \pi^*, \beta A^* - \gamma P \langle \pi_k, A_{k-1} - g(A_{k-1}) \rangle \rangle = \Delta_k^{\mathcal{H}g}$. When $\Delta_k^{\mathcal{H}g}$ is non-positive, it is guaranteed that $|\Delta_k^{\mathcal{H}g}| \leq |\Delta_k^{\mathcal{H}I}|$. In addition, we can expect that this error is largely decreased by zero function $g(x) \equiv 0$, though it makes harder to satisfy the inequality (11). However, this inequality does not always hold because it depends on the actual magnitude of A^* and $P \langle \pi_k, A_{k-1} - g(A_{k-1}) \rangle$.

Overall, there is a trade-off in the choice of g ; $g = I$ always satisfies the sufficient condition of asymptotic convergence (11), but the entropy term is not decreased. On the other hand, $g(x) \equiv 0$ is expected to decrease the entropy term, though which possibly violates (11) and might hinder the asymptotic performance. In the next section, we examine how the choice of f and g affects the empirical performance.

5 EXPERIMENT

5.1 BAL ON GRID WORLD

First, we compare the model-based tabular M-VI (2) and BAL (10). As discussed by Vieillard et al. (2020a), the larger the value of β is, the slower the initial convergence of MDVI gets, and thus M-VI as well. Since the inherent error reduction by BAL is effective when Ψ_k is far from optimum, it is expected that BAL is effective especially in earlier stage. We validate this hypothesis by a gridworld environment, where transition kernel P and reward function R are accessible. We performed 100 independent runs with random initialization of Ψ_0 . Figure 4 compares the normalized value of the suboptimality $\|V^{\pi_k} - V^*\|_\infty$, where the interquartile mean (IQM) is reported as suggested by Agarwal et al. (2021). The result suggests that BAL outperforms M-VI initially. Furthermore, $g \neq I$ performs slightly better than $g = I$ in the earlier stage, even in this toy problem. More experimental details are found in Appendix C.1.

5.2 MDAC ON MUJOCO LOCOMOTION ENVIRONMENTS

Setup and Metrics. Next, we empirically evaluate the effectiveness of MDAC on 6 Mujoco environments (Hopper-v4, HalfCheetah-v4, Walker2d-v4, Ant-v4, Humanoid-v4 and HumanoidStandup-v4) from Gymnasium (Towers et al., 2023). We evaluate our algorithm and baselines on 3M environmental steps, except for easier Hopper-v4 on 1M steps. For the reliable benchmarking, we again report the aggregated scores over all 6 environments as suggested by Agarwal et al. (2021). To be precise, we train 10 different instances of each algorithm with different random seeds and calculate baseline-normalized scores along iterations for each task as $\text{score} = \frac{\text{score}_{\text{algorithm}} - \text{score}_{\text{random}}}{\text{score}_{\text{baseline}} - \text{score}_{\text{random}}}$, where the baseline is the mean SAC score after 3M steps (1M for Hopper-v4). Then, we calculate the IQM score by aggregating the learning results over all 6 environments. We also report pointwise 95% percentile stratified bootstrap confidence intervals. We use Adam optimizer (Kingma & Ba, 2015) for all the gradient-based updates. The discount factor is set to $\gamma = 0.99$. All the function approximators, including those for baseline algorithms, are fully-connected feed-forward networks with two hidden layers and each hidden layer has 256 units with ReLU activations. We use a Gaussian policy with mean and standard deviation provided by the neural network. We fixed $\log \sigma_{\min} = -5$. More experimental details, including a full list of the hyperparameters and per-environment results, will be found in Appendix C.2.

Effect of bounding functions f and g . We start from evaluating how the performance of MDAC is affected by the choice of the bounding functions. First, we evaluate whether bounding both $\log \pi(a|s)$ terms is beneficial. We compare 3 choices: (i) $f = g = I$, (ii) $f(x) = \tanh(x/10)$, $g = I$ and (iii) $f(x) = g(x) = \tanh(x/10)$. Figure 5 compares the learning results for these choices and it indicates that bounding both $\alpha \log \pi$ terms is indeed beneficial.

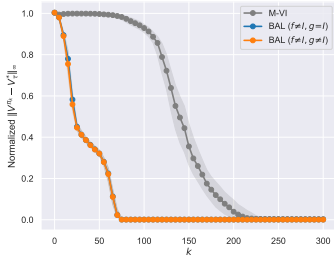


Figure 4: Comparison of M-VI and BAL.

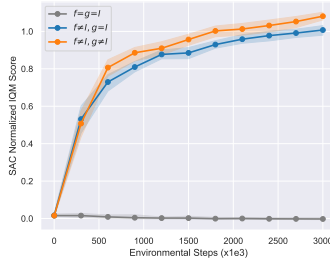


Figure 5: Effect of $f \neq I$ and $g \neq I$.

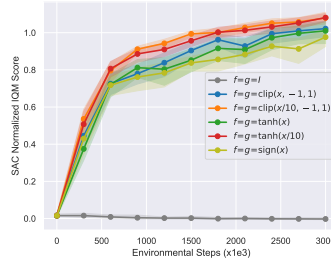


Figure 6: Comparison of f and g .

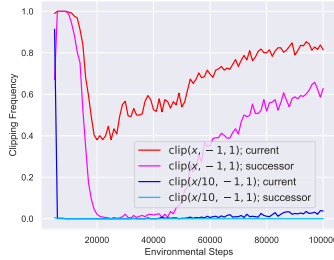


Figure 7: Clipping frequencies.

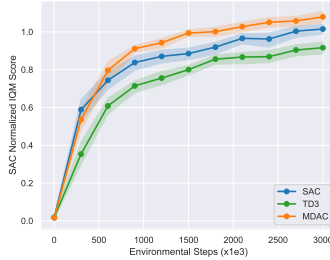


Figure 8: Comparison on Mujoco.

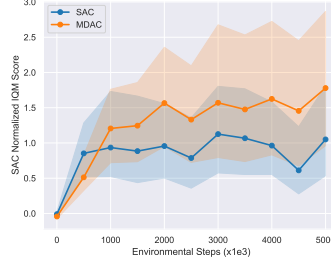


Figure 9: Comparison on dog domains.

Next, we compare 5 choices under $f = g \neq I$: (i) $\text{clip}(x, -1, 1)$, (ii) $\text{clip}(x/10, -1, 1)$, (iii) $\text{tanh}(x)$, (iv) $\text{tanh}(x/10)$, and (v) $\text{sign}(x)$. Notice that the last choice (v) violates our requirement to the bounding functions. Figure 6 compares the learning curves for the choice (iii) and (iv). The result indicates that the performance difference between $\text{clip}(x)$ and $\text{tanh}(x)$ is small. On the other hand, the performance is better if the slower saturating functions are used. Furthermore, $\text{sign}(x)$ resulted in the worst performance among these choices. Figure 7 compares the frequencies of clipping $\alpha \log \pi$ terms by $\text{clip}(x, -1, 1)$ and $\text{clip}(x/10, -1, 1)$ in the sampled minibatches for the initial learning phase in `HalfCheetah-v4`. For $\text{clip}(x, -1, 1)$, the clipping occurs frequently especially for the current (s, a) pairs and the information of relative $\alpha \log \pi$ values between different state-actions are lost. In contrast, for $\text{clip}(x/10, -1, 1)$, the clipping rarely happens and the information of relative $\alpha \log \pi$ values are leveraged in the learning. These results suggest that the relative values of $\alpha \log \pi$ terms between different state-actions are beneficial, even though the raw values (by $f = g = I$) are harmful.

Comparison to baseline algorithms. We compare MDAC against SAC (Haarnoja et al., 2018b), an entropy-only-regularized method, and TD3 (Fujimoto et al., 2018), a non-regularized method. We adopted $f(x) = g(x) = \text{clip}(x/10, -1, 1)$. Figure 8 compares the learning results. Notice that the final IQM score of SAC does not match 1, because the scores are normalized by the mean of all the SAC runs, whereas IQM is calculated by middle 50% runs. The results show that MDAC overtakes both SAC and TD3.

5.3 MDAC ON DEEPMIND CONTROL SUITE

Finally, we compare MDAC and SAC on the challenging `dog` domain from DeepMind Control Suite (Tunyasuvunakool et al., 2020). We adopted `stand`, `walk`, `trot`, `run` and `fetch` tasks. We train 30 different instances of each algorithm for 5M environmental steps, and report SAC normalized IQM scores. We adopted $f(x) = g(x) = \text{clip}(x/10, -1, 1)$ for MDAC again. Hyperparameters are set to equivalent values as in Mujoco experiments. Figure 9 compares the aggregated learning results. Though the aggregated result is not very strong statistically, MDAC tends to reach better performance than SAC. Figure 10 shows per-environment results with 25% and 75% percentile scores. While the performances of SAC often degrade during the learning due to the difficulty of the `dog` domain, this degradation is less observed for MDAC. We conjecture that this effect is due to the implicit KL-regularized nature of MDAC.

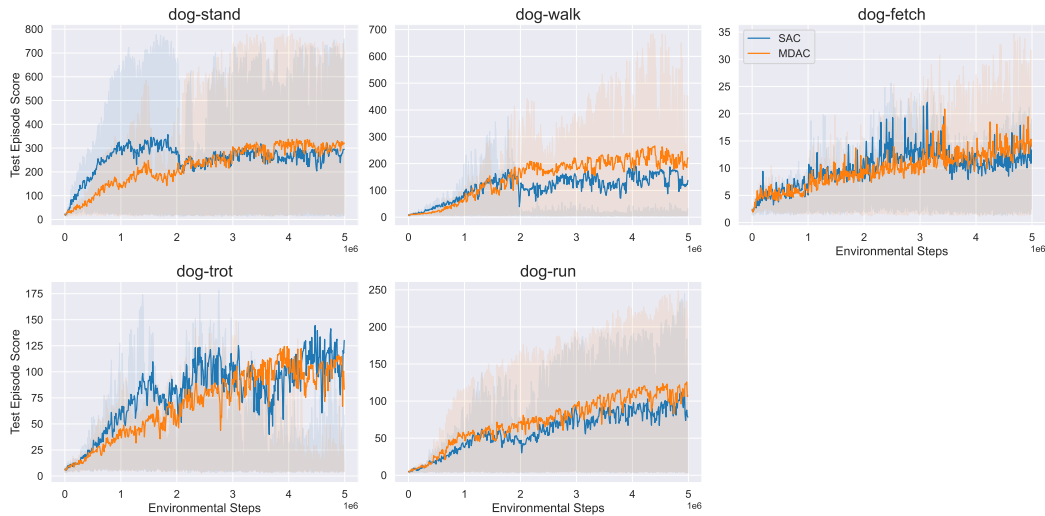


Figure 10: Per-environment performances in `dog` domain from DeepMind Control Suite. The mean scores of 30 independent runs are reported. The shaded region corresponds to 25% and 75% percentile scores over the 30 runs.

6 CONCLUSION

In this study, we proposed MDAC, a model-free actor-critic instantiation of MDVI for continuous action domains. We showed that its empirical performance is significantly boosted by bounding the values of log-density terms in the critic loss. By relating MDAC to AL, we theoretically showed that the inherent error of gap-increasing operators is decreased by bounding the soft advantage terms, as well as provided the convergence analyses. Our analyses indicated that bounding both of the log-policy terms is beneficial. Lastly, we evaluated the effectiveness of MDAC empirically in simulated environments.

Limitations. This study has three major limitations. Firstly, our theoretical analyses are valid only for fixed α . Thus, its exploding behavior observed in Section 3 for $f = g = I$ is not captured. Secondly, our theoretical analyses apply only to tabular cases in the current forms. To extend our analyses to continuous state-action domains, we need measure-theoretic considerations as explored in Appendix B of (Puterman, 1994). Lastly, our analyses and experiments do not offer the optimal design of the bounding functions f and g . We leave these issues as open questions.

REFERENCES

- Abbas Abdolmaleki, Jost Tobias Springenberg, Yuval Tassa, Remi Munos, Nicolas Heess, and Martin Riedmiller. Maximum a posteriori policy optimisation. In *International Conference on Learning Representations*, 2018. 1
- Joshua Achiam. Spinning Up in Deep Reinforcement Learning. 2018. 2, 4
- Rishabh Agarwal, Max Schwarzer, Pablo Samuel Castro, and Marc G. Bellemare. Deep reinforcement learning at the edge of the statistical precipice. In *35th Conference on Neural Information Processing Systems*, 2021. 9
- Carlo Alfano, Rui Yuan, and Patrick Rebeschini. A novel framework for policy mirror descent with general parameterization and linear convergence. In *Thirty-seventh Conference on Neural Information Processing Systems*, 2023. 2, 14

- András Antos, Csaba Szepesvári, and Rémi Munos. Learning near-optimal policies with bellman-residual minimization based fitted policy iteration and a single sample path. *Machine Learning*, 71:89–129, 2008. [8](#)
- Mohammad Gheshlaghi Azar, Vicenç Gómez, and Hilbert J. Kappen. Dynamic policy programming. *Journal of Machine Learning Research*, 13, 2012. [1](#)
- Leemon C. Baird. *Reinforcement learning through gradient descent*. PhD thesis, Ph.D. Dissertation, Carnegie Mellon University, 1999. [1](#), [5](#)
- R Basu, V Kannan, K Sannyasi, and N Unnikrishnan. Functions preserving limit superior. *The College Mathematics Journal*, 50(1):58–60, 2019. [16](#)
- Marc G. Bellemare, Georg Ostrovski, Arthur Guez, Philip S. Thomas, and Rémi Munos. Increasing the action gap: New operators for reinforcement learning. In *Proceedings of the 30th Conference on Artificial Intelligence (AAAI-16)*, 2016. [1](#), [5](#), [7](#), [16](#)
- Richard Bellman and Stuart Dreyfus. Functional approximations and dynamic programming. *Mathematics of Computation*, 13(68):247–251, 1959. [3](#)
- Jonas Degraeve, Federico Felici, Jonas Buchli, Michael Neunert, Brendan Tracey, Francesco Carpanese, Timo Ewalds, Roland Hafner, Abbas Abdolmaleki, Diego de Las Casas, et al. Magnetic control of tokamak plasmas through deep reinforcement learning. *Nature*, 602(7897):414–419, 2022. [1](#)
- Amir-massoud Farahmand. Action-gap phenomenon in reinforcement learning. In J. Shawe-Taylor, R. Zemel, P. Bartlett, F. Pereira, and K.Q. Weinberger (eds.), *Advances in Neural Information Processing Systems*, volume 24. Curran Associates, Inc., 2011. [7](#), [16](#)
- Amir-massoud Farahmand, Csaba Szepesvári, and Rémi Munos. Error propagation for approximate policy and value iteration. In *Advances in Neural Information Processing Systems 23*, 2010. [8](#)
- Scott Fujimoto, Herke van Hoof, and David Meger. Addressing function approximation error in actor-critic methods. In Jennifer Dy and Andreas Krause (eds.), *Proceedings of the 35th International Conference on Machine Learning*, volume 80 of *Proceedings of Machine Learning Research*, pp. 1587–1596. PMLR, 10–15 Jul 2018. [2](#), [10](#)
- Matthieu Geist, Bruno Scherrer, and Olivier Pietquin. A theory of regularized markov decision processes. In *Proceedings of The 36th International Conference on Machine Learning*, 2019. [1](#), [3](#)
- Tuomas Haarnoja, Haoran Tang, Pieter Abbeel, and Sergey Levine. Reinforcement learning with deep energy-based policies. In *Proceedings of The 34th International Conference on Machine Learning*, pp. 1352–1361, 2017. [1](#)
- Tuomas Haarnoja, Aurick Zhou, Pieter Abbeel, and Sergey Levine. Soft actor-critic: Off-policy maximum entropy deep reinforcement learning with a stochastic actor. In *Proceedings of The 35th International Conference on Machine Learning*, pp. 1861–1870, 2018a. [1](#), [4](#)
- Tuomas Haarnoja, Aurick Zhou, Kristian Hartikainen, George Tucker, Sehoon Ha, Jie Tan, Vikash Kumar, Henry Zhu, Abhishek Gupta, Pieter Abbeel, and Sergey Levine. Soft actor-critic algorithms and applications. In *arXiv*, 2018b. [4](#), [10](#)
- Shengyi Huang, Rousslan Fernand Julien Dossa, Chang Ye, Jeff Braga, Dipam Chakraborty, Kinal Mehta, and João G.M. Araújo. Cleanrl: High-quality single-file implementations of deep reinforcement learning algorithms. *Journal of Machine Learning Research*, 23(274): 1–18, 2022. [2](#), [4](#)
- Ryo Iwaki and Minoru Asada. Implicit incremental natural actor critic algorithm. *Neural Networks*, 109:103–112, 2019. [2](#)
- Sham Kakade. A natural policy gradient. In *Advances in Neural Information Processing Systems 14*, pp. 227–242, 2001. [2](#)

- Diederik P. Kingma and Jimmy Lei Ba. Adam: A method for stochastic optimization. In *International Conference for Learning Representations*, 2015. [9](#), [24](#)
- Tadashi Kozuno, Eiji Uchibe, and Kenji Doya. Theoretical analysis of efficiency and robustness of softmax and gap-increasing operators in reinforcement learning. In *Proceedings of the Twenty-Second International Conference on Artificial Intelligence and Statistics*, volume 89 of *Proceedings of Machine Learning Research*, pp. 2995–3003. PMLR, 2019. [8](#)
- Tadashi Kozuno, Wenhao Yang, Nino Vieillard, Toshinori Kitamura, Yunhao Tang, Jincheng Mei, Pierre M enard, Mohammad Gheshlaghi Azar, Michal Valko, R emi Munos, Olivier Pietquin, Matthieu Geist, and Csaba Szepesv ari. Kl-entropy-regularized rl with a generative model is minimax optimal. In *arXiv*, 2022. [1](#), [4](#)
- Jakub Grudzien Kuba, Christian A Schroeder De Witt, and Jakob Foerster. Mirror learning: A unifying framework of policy optimisation. In *Proceedings of the 39th International Conference on Machine Learning*, volume 162, pp. 7825–7844. PMLR, 2022. [2](#), [14](#)
- Guanghui Lan. Policy mirror descent for reinforcement learning: Linear convergence, new sampling complexity, and generalized problem classes. *Mathematical programming*, 198(1): 1059–1106, 2023. [2](#), [14](#)
- R emi Munos. Error bounds for approximate value iteration. In *Proceedings of the National Conference on Artificial Intelligence*, volume 20, pp. 1006. Menlo Park, CA; Cambridge, MA; London; AAAI Press; MIT Press; 1999, 2005. [8](#)
- R emi Munos. Performance bounds in l_p -norm for approximate value iteration. *SIAM journal on control and optimization*, 46(2):541–561, 2007. [8](#)
- Jan Peters, Katharina M ulling, and Yasemin Alt un. Relative entropy policy search. In *AAAI Conference on Artificial Intelligence*, 2010. [1](#)
- Martin L. Puterman. *Markov Decision Processes: Discrete Stochastic Dynamic Programming*. Wiley, 1994. [11](#)
- John Schulman, Sergey Levine, Philipp Moritz, Michael Jordan, and Pieter Abbeel. Trust region policy optimization. In *Proceedings of the 32nd International Conference on Machine Learning*, pp. 1889–1897, 2015. [1](#)
- John Schulman, Filip Wolski, Prafulla Dhariwal, Alec Radford, and Oleg Klimov. Proximal policy optimization algorithms. In *arXiv*, volume 1707.06347, 2017. [1](#)
- David Silver, Guy Lever, Nicolas Heess, Thomas Degris, Daan Wierstra, and Martin Riedmiller. Deterministic policy gradient algorithms. *Proceedings of the 31st International Conference on Machine Learning*, pp. 387–395, 2014. [2](#)
- Laura Smith, Ilya Kostrikov, and Sergey Levine. Demonstrating a walk in the park: Learning to walk in 20 minutes with model-free reinforcement learning. In *Robotics: Science and System XIX*, 2023. [1](#)
- Nisan Stiennon, Long Ouyang, Jeffrey Wu, Daniel Ziegler, Ryan Lowe, Chelsea Voss, Alec Radford, Dario Amodei, and Paul F Christiano. Learning to summarize with human feedback. In H. Larochelle, M. Ranzato, R. Hadsell, M.F. Balcan, and H. Lin (eds.), *Advances in Neural Information Processing Systems*, volume 33, pp. 3008–3021, 2020. [1](#)
- Philip S Thomas, William C Dabney, Stephen Giguere, and Sridhar Mahadevan. Projected natural actor-critic. *Advances in neural information processing systems*, 26, 2013. [2](#)
- Manan Tomar, Lior Shani, Yonathan Efroni, and Mohammad Ghavamzadeh. Mirror descent policy optimization. In *International Conference on Learning Representations*, 2022. [2](#), [14](#)
- Mark Towers, Jordan K. Terry, Ariel Kwiatkowski, John U. Balis, Gianluca de Cola, Tristan Deleu, Manuel Goul ao, Andreas Kallinteris, Arjun KG, Markus Krimmel, Rodrigo Perez-Vicente, Andrea Pierr e, Sander Schulhoff, Jun Jet Tai, Andrew Tan Jin Shen, and Omar G. Younis. Gymnasium, March 2023. URL <https://zenodo.org/record/8127025>. [9](#)

- Saran Tunyasuvunakool, Alistair Muldal, Yotam Doron, Siqu Liu, Steven Bohez, Josh Merel, Tom Erez, Timothy Lillicrap, Nicolas Heess, and Yuval Tassa. `dm.control`: Software and tasks for continuous control. *Software Impacts*, 6:100022, 2020. ISSN 2665-9638. doi: <https://doi.org/10.1016/j.simpa.2020.100022>. URL <https://www.sciencedirect.com/science/article/pii/S2665963820300099>. 10
- Harm van Seijen, Hado van Hasselt, Shimon Whiteson, and Marco Wiering. A theoretical and empirical analysis of expected sarsa. In *2009 IEEE Symposium on Adaptive Dynamic Programming and Reinforcement Learning*, pp. 177–184, 2009. doi: 10.1109/ADPRL.2009.4927542. 6
- Sharan Vaswani, Olivier Bachem, Simone Totaro, Robert Müller, Shivam Garg, Matthieu Geist, Marlos C. Machado, Pablo Samuel Castro, and Nicolas Le Roux. A general class of surrogate functions for stable and efficient reinforcement learning. In *Proceedings of The 25th International Conference on Artificial Intelligence and Statistics*, volume 151, pp. 8619–8649. PMLR, 2022. 2, 14
- Nino Vieillard, Tadashi Kozuno, Bruno Scherrer, Olivier Pietquin, Rémi Munos, and Matthieu Geist. Leverage the average: an analysis of kl regularization in reinforcement learning. In *Advances in Neural Information Processing Systems*, 2020a. 1, 3, 6, 8, 9
- Nino Vieillard, Olivier Pietquin, and Matthieu Geist. Munchausen reinforcement learning. In *Advances in Neural Information Processing Systems*, 2020b. 1, 2, 3, 4, 7, 14
- Nino Vieillard, Marcin Andrychowicz, Anton Raichuk, Olivier Pietquin, and Matthieu Geist. Implicitly regularized rl with implicit q-values. In *Proceedings of the 25th International Conference on Artificial Intelligence and Statistics*, 2022. 1, 2
- Qing Wang, Yingru Li, Jiechao Xiong, and Tong Zhang. Divergence-augmented policy optimization. In *Advances in Neural Information Processing Systems*, volume 32. Curran Associates, Inc., 2019. 2, 14
- Long Yang, Yu Zhang, Gang Zheng, Qian Zheng, Pengfei Li, Jianhang Huang, and Gang Pan. Policy optimization with stochastic mirror descent. In *Proceedings of the AAAI Conference on Artificial Intelligence*, volume 36, pp. 8823–8831, 2022. 2, 14
- Zhe Zhang, Yaozhong Gan, and Xiaoyang Tan. Robust action gap increasing with clipped advantage learning. In *Proceedings of the 36th Conference on Artificial Intelligence (AAAI-2)*, 2022. 2, 8

A ADDITIONAL DISCUSSION ON MD-BASED RL METHODS

Wang et al. (2019) explores off-policy policy gradients in MD view and proposes an off-policy variant of PPO. Tomar et al. (2022) considers a MD structure with the advantage function and the KL divergence, and proposes variants of SAC and PPO. Yang et al. (2022) incorporates a variance reduction method into MD based RL. Vaswani et al. (2022) and Alfano et al. (2023) try to generalize the existing MD based approaches to general policy parameterizations. Kuba et al. (2022) proposes a further generalization that unify even non-regularized RL methods such as DDPG and A3C. Lan (2023) proposes a MD method that resembles MDVI, which incorporates both the (Bregman/KL) divergence and an additional convex regularizer, and show that it achieves fast linear rate of convergence. Munchausen RL is distinct from the above literature in the sense that, it is *implicit* mirror descent due to the sound reparameterization by Vieillard et al. (2020b). Though this makes it very easy to implement, the control of the policy change is vague, particularly when combined with function approximations. Thus, we argue that (1) Munchausen RL based methods are very good starting point to use, and (2) if a precise control of policy change is demanded, another MD methods could be tried.

B PROOFS

B.1 BASIC PROPERTIES OF \mathbb{L}^α

In this section, we omit Ψ 's dependency to state s , and let $\Psi \in \mathbb{R}^{\mathcal{A}}$ for brevity. For $\alpha > 0$, we write $\mathbb{L}^\alpha \Psi = \alpha \log \langle \mathbf{1}, \exp \frac{\Psi}{\alpha} \rangle \in \mathbb{R}$.

Lemma 1. \mathbb{L}^α is continuous and strictly increasing.

Proof. Continuity follows from the fact that $\mathbb{L}^\alpha \Psi = \alpha \log \langle \mathbf{1}, \exp \frac{\Psi}{\alpha} \rangle$ is a composition of continuous functions. We also have that

$$\frac{\partial}{\partial \Psi(a)} \mathbb{L}^\alpha \Psi = \frac{\exp \frac{\Psi(a)}{\alpha}}{\langle \mathbf{1}, \exp \frac{\Psi}{\alpha} \rangle} > 0,$$

from which we conclude that \mathbb{L}^α is strictly increasing. ■

Lemma 2. It holds that

$$\max_{a \in \mathcal{A}} \Psi(a) \leq \mathbb{L}^\alpha \Psi \leq \max_{a \in \mathcal{A}} \Psi(a) + \alpha \log |\mathcal{A}|.$$

Proof. Let $y = \max_{a \in \mathcal{A}} \Psi(a)$. We have that

$$\exp \frac{y}{\alpha} \leq \langle \mathbf{1}, \exp \frac{\Psi}{\alpha} \rangle = \sum_{a \in \mathcal{A}} \exp \frac{\Psi(a)}{\alpha} \leq |\mathcal{A}| \exp \frac{y}{\alpha}.$$

Applying the logarithm to this inequality, we have

$$\frac{y}{\alpha} \leq \log \langle \mathbf{1}, \exp \frac{\Psi}{\alpha} \rangle \leq \frac{y}{\alpha} + \log |\mathcal{A}|,$$

and thus the claim follows. ■

Lemma 3. It holds that $\lim_{\alpha \rightarrow 0} \mathbb{L}^\alpha \Psi \rightarrow \max_{a \in \mathcal{A}} \Psi(a)$.

Proof. Let $y = \max_{a \in \mathcal{A}} \Psi(a)$ and $\mathcal{B} = \{a \in \mathcal{A} | \Psi(a) = y\}$. It holds that

$$\begin{aligned} \mathbb{L}^\alpha \Psi &= \alpha \log \sum_{a \in \mathcal{A}} \exp \frac{\Psi(a)}{\alpha} \\ &= \alpha \log \left(\exp \frac{y}{\alpha} \sum_{a \in \mathcal{A}} \exp \frac{\Psi(a) - y}{\alpha} \right) \\ &= y + \alpha \log \left(\underbrace{\sum_{a \in \mathcal{B}} \exp \frac{\Psi(a) - y}{\alpha}}_{=1} + \sum_{a \notin \mathcal{B}} \exp \frac{\Psi(a) - y}{\alpha} \right) \\ &= y + \alpha \log \left(|\mathcal{B}| + \sum_{a \notin \mathcal{B}} \exp \frac{\Psi(a) - y}{\alpha} \right). \end{aligned}$$

Since $\Psi(a) - y < 0$ for $a \notin \mathcal{B}$, we have $\exp \frac{\Psi(a) - y}{\alpha} \rightarrow 0$ as $\alpha \rightarrow 0$ for $a \notin \mathcal{B}$, thus it holds that $\lim_{\alpha \rightarrow 0} \mathbb{L}^\alpha \Psi \rightarrow y = \max_{a \in \mathcal{A}} \Psi(a)$. ■

Lemma 4. Let v be independent of actions. Then it holds that $\mathbb{L}^\alpha(\Psi + v) = \mathbb{L}^\alpha(\Psi) + v$.

Proof.

$$\mathbb{L}^\alpha(\Psi + v) = \alpha \log \left\langle \mathbf{1}, \exp \frac{\Psi + v}{\alpha} \right\rangle = \alpha \log \left\langle \mathbf{1}, \exp \frac{\Psi}{\alpha} \right\rangle + \alpha \log \exp \frac{v}{\alpha} = \mathbb{L}^\alpha \Psi + v. ■$$

Lemma 5. *It holds that $\mathbb{L}^\alpha \frac{1}{1-\beta} \Psi = \frac{1}{1-\beta} \mathbb{L}^\tau \Psi$.*

Proof. Noticing $\tau = (1 - \beta)\alpha$, we have

$$\mathcal{G}^{0,\alpha} \left(\frac{\Psi}{1-\beta} \right) = \frac{\exp \frac{1}{\alpha} \frac{\Psi}{1-\beta}}{\left\langle \mathbf{1}, \exp \frac{1}{\alpha} \frac{\Psi}{1-\beta} \right\rangle} = \frac{\exp \frac{\Psi}{\tau}}{\left\langle \mathbf{1}, \exp \frac{\Psi}{\tau} \right\rangle} = \mathcal{G}^{0,\tau}(\Psi) =: \pi_\tau,$$

and thus

$$\mathbb{L}^\alpha \frac{\Psi}{1-\beta} = \left\langle \pi_\tau, \frac{\Psi}{1-\beta} \right\rangle + \alpha \mathcal{H}(\pi_\tau) = \frac{1}{1-\beta} (\langle \pi_\tau, \Psi \rangle + (1-\beta)\alpha \mathcal{H}(\pi_\tau)) = \frac{1}{1-\beta} \mathbb{L}^\tau \Psi. \quad \blacksquare$$

Lemma 6. *Let $(\Psi_k)_{k \in \mathbb{N}}$ be a bounded sequence. Then it holds that, for pointwise,*

$$\limsup_{k \rightarrow \infty} \mathbb{L}^\alpha \Psi_k \leq \mathbb{L}^\alpha \limsup_{k \rightarrow \infty} \Psi_k$$

and

$$\mathbb{L}^\alpha \liminf_{k \rightarrow \infty} \Psi_k \leq \liminf_{k \rightarrow \infty} \mathbb{L}^\alpha \Psi_k.$$

Proof. Since log and exp are continuous and strictly increasing, lim sup and lim inf are both commute with these functions (Basu et al., 2019). Furthermore, for real valued bounded sequences x_k and y_k , we have $\limsup_{k \rightarrow \infty} (x_k + y_k) \leq \limsup_{k \rightarrow \infty} x_k + \limsup_{k \rightarrow \infty} y_k$ and $\liminf_{k \rightarrow \infty} x_k + \liminf_{k \rightarrow \infty} y_k \leq \liminf_{k \rightarrow \infty} (x_k + y_k)$. Since \mathbb{L}^α is a composition of exp, summation and log, the claim follows. \blacksquare

B.2 ASYMPTOTIC PROPERTY OF BAL WITH $\alpha \rightarrow 0$

If an action-value function is updated using an operator \mathcal{T}' that is *optimality-preserving*, at least one optimal action remains optimal, and suboptimal actions remain suboptimal. Further, if the operator \mathcal{T}' is also *gap-increasing*, the value of suboptimal actions are pushed-down, which is advantageous in the presence of approximation or estimation errors (Farahmand, 2011).

Now, we provide the formal definitions of *optimality-preserving* and *gap-increasing*.

Definition 1 (Optimality-preserving). *An operator \mathcal{T}' is optimality-preserving if, for any $Q_0 \in \mathbb{R}^{\mathcal{S} \times \mathcal{A}}$ and $s \in \mathcal{S}$, letting $Q_{k+1} := \mathcal{T}' Q_k$, $\tilde{V}(s) := \lim_{k \rightarrow \infty} \max_{b \in \mathcal{A}} Q_k(s, b)$ exists, is unique, $\tilde{V}(s) = V^*(s)$, and for all $a \in \mathcal{A}$, $Q^*(s, a) < V^*(s, a) \implies \limsup_{k \rightarrow \infty} Q_k(s, a) < V^*(s)$.*

Definition 2 (Gap-increasing). *An operator \mathcal{T}' is gap-increasing if for all $Q_0 \in \mathbb{R}^{\mathcal{S} \times \mathcal{A}}$, $s \in \mathcal{S}, a \in \mathcal{A}$, letting $Q_{k+1} := \mathcal{T}' Q_k$ and $V_k(x) := \max_b Q_k(s, b)$, $\liminf_{k \rightarrow \infty} [V_k(s) - Q_k(s, a)] \geq V^*(s) - Q^*(s, a)$.*

The following lemma characterizes the conditions when an operator is optimality-preserving and gap-increasing.

Lemma 7 (Theorem 1 in (Bellemare et al., 2016)). *Let $V(s) := \max_b Q(s, b)$ and let \mathcal{T} be the Bellman optimality operator $\mathcal{T}Q = R + \gamma PV$. Let \mathcal{T}' be an operator with the property that there exists an $\rho \in [0, 1)$ such that for all $Q \in \mathbb{R}^{\mathcal{S} \times \mathcal{A}}$, $s \in \mathcal{S}, a \in \mathcal{A}$, $\mathcal{T}'Q \leq \mathcal{T}Q$, and $\mathcal{T}'Q \geq \mathcal{T}Q - \rho(V - Q)$. Then \mathcal{T}' is both optimality-preserving and gap-increasing.*

Notably, our operator $\mathcal{T}_{\pi_{k+1}}^{fg}$ is both optimality-preserving and gap-increasing in the limit $\alpha \rightarrow 0$.

Theorem 3. *In the limit $\alpha \rightarrow 0$, the operator $\mathcal{T}_{\pi_{k+1}}^{fg}$ satisfies $\mathcal{T}_{\pi_{k+1}}^{fg} \Psi_k \leq \mathcal{T} \Psi_k$ and $\mathcal{T}_{\pi_{k+1}}^{fg} \Psi_k \geq \mathcal{T} \Psi_k - \beta (V_k - \Psi_k)$ and thus is both optimality-preserving and gap-increasing.*

Proof. From Lemma 3, we have $\mathbb{L}^\alpha(s)\Psi \rightarrow \max_{a \in \mathcal{A}} \Psi(s, a)$ as $\alpha \rightarrow 0$ for $\Psi \in \mathbb{R}^{\mathcal{S} \times \mathcal{A}}$. Observe that, for $h \in \{f, g\}$, it holds that $h(A_k) = h(\Psi_k - V_k) \leq 0$ since $A_k(s, a) = \Psi_k(s, a) - \max_{b \in \mathcal{A}} \Psi_k(s, b) \leq 0$ and h does not flip the sign of argument. Additionally, for $\pi_{k+1} \in \mathcal{G}(\Psi_k)$ it follows that $\langle \pi_{k+1}, h(A_k) \rangle = 0$ since $h(0) = 0$. It holds that

$$\begin{aligned} \mathcal{T}_{\pi_{k+1}}^{fg} \Psi_k - \mathcal{T} \Psi_k &= R + \beta f(A_k) + \gamma P \langle \pi_{k+1}, \Psi_k - g(A_k) \rangle - R - \gamma P \langle \pi_{k+1}, \Psi_k \rangle \\ &= \beta \underbrace{f(A_k)}_{\leq 0} - \gamma P \underbrace{\langle \pi_{k+1}, g(A_k) \rangle}_{=0} \leq 0. \end{aligned}$$

Furthermore, observing that $x - f(x) \leq 0$ for $x \leq 0$, it follows that

$$\mathcal{T}_{\pi_{k+1}}^{fg} \Psi_k - \mathcal{T} \Psi_k + \beta (V_k - \Psi_k) = -\beta \underbrace{(A_k - f(A_k))}_{\leq 0} - \gamma P \underbrace{\langle \pi_{k+1}, g(A_k) \rangle}_{=0} \geq 0.$$

Thus, the operator $\mathcal{T}_{\pi_{k+1}}^{fg}$ satisfies the conditions of Lemma 7. Therefore we conclude that $\mathcal{T}_{\pi_{k+1}}^{fg}$ is both optimality-preserving and gap-increasing. \blacksquare

B.3 PROOF OF THEOREM 1

We provide several lemmas that are used to prove Theorem 1.

Lemma 8. *Let $\Psi \in \mathbb{R}^{\mathcal{S} \times \mathcal{A}}$, $V = \mathbb{L}^\alpha \Psi$ and \mathcal{T}' be an operator with the properties that $\mathcal{T}' \Psi \leq \mathcal{T}^\alpha \Psi$ and $\mathcal{T}' \Psi \geq \mathcal{T}^\alpha \Psi - \beta (V - \Psi) = \mathcal{T}^\alpha \Psi + \beta (A)$. Consider the sequence $\Psi_{k+1} := \mathcal{T}' \Psi_k$ with $\Psi_0 \in \mathbb{R}^{\mathcal{S} \times \mathcal{A}}$, and let $V_k = \mathbb{L}^\alpha \Psi_k$. Then the sequence $(V_k)_{k \in \mathbb{N}}$ converges.*

Proof.

$$\begin{aligned} V_{k+1} &= \mathbb{L}^\alpha \Psi_{k+1} = \langle \pi_{k+2}, \Psi_{k+1} \rangle + \alpha \mathcal{H}(\pi_{k+2}) \\ &\geq \langle \pi_{k+1}, \Psi_{k+1} \rangle + \alpha \mathcal{H}(\pi_{k+1}) \\ &= \langle \pi_{k+1}, \mathcal{T}' \Psi_k \rangle + \alpha \mathcal{H}(\pi_{k+1}) \\ &\geq \langle \pi_{k+1}, \mathcal{T}^\alpha \Psi_k + \beta A_k \rangle + \alpha \mathcal{H}(\pi_{k+1}) \\ &\stackrel{(a)}{=} \langle \pi_{k+1}, \mathcal{T}^\alpha \Psi_k \rangle + (1 - \beta) \alpha \mathcal{H}(\pi_{k+1}) \\ &\stackrel{(b)}{=} \langle \pi_{k+1}, Q_k + \gamma P(V_k - V_{k-1}) \rangle + (1 - \beta) \alpha \mathcal{H}(\pi_{k+1}) \\ &\stackrel{(c)}{=} \langle \pi_{k+1}, Q_k + \gamma P(V_k - V_{k-1}) \rangle + \tau \mathcal{H}(\pi_{k+1}) - \lambda D_{\text{KL}}(\pi_{k+1} \| \pi_k) + \lambda D_{\text{KL}}(\pi_{k+1} \| \pi_k) \\ &\stackrel{(d)}{=} V_k + \langle \pi_{k+1}, \gamma P(V_k - V_{k-1}) \rangle + \lambda D_{\text{KL}}(\pi_{k+1} \| \pi_k) \\ &\geq V_k + \langle \pi_{k+1}, \gamma P(V_k - V_{k-1}) \rangle, \end{aligned}$$

where (a) follows from $\langle \pi_{k+1}, A_k \rangle = \langle \pi_{k+1}, \alpha \log \pi_{k+1} \rangle = -\alpha \mathcal{H}(\pi_{k+1})$, (b) follows from $\mathcal{T}^\alpha \Psi_k = R + \gamma P \mathbb{L}^\alpha \Psi_k = R + \gamma P V_k = Q_{k+1}$, (c) follows from $(1 - \beta) \alpha = \tau$, and (d) follows from $V_k = \mathbb{L}^\alpha \Psi_k = \langle \pi_{k+1}, Q_k \rangle + \tau \mathcal{H}(\pi_{k+1}) - \lambda D_{\text{KL}}(\pi_{k+1} \| \pi_k)$. Thus we have

$$V_{k+1} - V_k \geq \gamma P^{\pi_{k+1}} (V_k - V_{k-1})$$

and by induction

$$V_{k+1} - V_k \geq \gamma^k P_{k+1:2} (V_1 - V_0),$$

where $P_{k+1:2} = P^{\pi_{k+1}} P^{\pi_k} \dots P^{\pi_2}$. From the conditions on \mathcal{T}' , if V_0 is bounded then V_1 is also bounded, and thus $\|V_1 - V_0\|_\infty < \infty$. By definition, for any $\delta > 0$ and $n \in \mathbb{N}$, $\exists k \geq n$ such that $V_k > \tilde{V} - \delta$. Since $P_{k+1:2}$ is a nonexpansion in ∞ -norm, we have

$$V_{k+1} - V_k \geq -\gamma^k \|V_1 - V_0\|_\infty \geq -\gamma^n \|V_1 - V_0\|_\infty =: -\epsilon,$$

and for all $t \in \mathbb{N}$,

$$V_{k+t} - V_k \geq -\sum_{i=0}^{t-1} \gamma^i \epsilon \geq \frac{-\epsilon}{1 - \gamma}.$$

Thus, we have

$$\inf_{t \in \mathbb{N}} V_{k+t} \geq V_k - \frac{\epsilon}{1-\gamma} > \tilde{V} - \delta - \frac{\epsilon}{1-\gamma}.$$

It follows that for any $\delta' > 0$, we can choose an $n \in \mathbb{N}$ to make ϵ small enough such that for all $k \geq n$, $V_k > \tilde{V} - \delta'$. Hence

$$\liminf_{k \rightarrow \infty} V_k = \tilde{V},$$

and thus V_k converges. \blacksquare

Lemma 9. *Let \mathcal{T}' be an operator satisfying the conditions of Lemma 8. Then for all $k \in \mathbb{N}$,*

$$|V_k| \leq \frac{1}{1-\gamma} \left(R_{\max} + 3 \|V_0\|_{\infty} + \alpha \log |\mathcal{A}| \right) =: V_{\max}^{\text{SGI}}. \quad (13)$$

Proof. Following the derivation of Lemma 8, we have

$$V_{k+1} - V_0 \geq - \sum_{i=1}^k \gamma^i \|V_1 - V_0\|_{\infty} \geq \frac{-1}{1-\gamma} \|V_1 - V_0\|_{\infty}. \quad (14)$$

We also have

$$V_1 = \mathbb{L}^{\alpha} \mathcal{T}' \Psi_0 \leq \mathbb{L}^{\alpha} \mathcal{T}^{\alpha} \Psi_0 = \max \langle \pi, R + \gamma P V_0 \rangle + \alpha \mathcal{H}(\pi) \leq \|R + \gamma P V_0\|_{\infty} + \alpha \log |\mathcal{A}|$$

and then for pointwise

$$V_1 - V_0 \leq R_{\max} + 2 \|V_0\|_{\infty} + \alpha \log |\mathcal{A}|.$$

Combining above and (14), we have

$$V_{k+1} \geq V_0 - \frac{1}{1-\gamma} (R_{\max} + 2 \|V_0\|_{\infty} + \alpha \log |\mathcal{A}|) \quad (15)$$

$$\geq -\frac{1-\gamma}{1-\gamma} \|V_0\|_{\infty} - \frac{1}{1-\gamma} (R_{\max} + 2 \|V_0\|_{\infty} + \alpha \log |\mathcal{A}|) \quad (16)$$

$$\geq -\frac{1}{1-\gamma} (3 \|V_0\|_{\infty} + R_{\max} + \alpha \log |\mathcal{A}|). \quad (17)$$

Now assume that the upper bound of (13) holds up to $k \in \mathbb{N}$. Then we have

$$\begin{aligned} V_{k+1} &= \mathbb{L}^{\alpha} \mathcal{T}' \Psi_k \leq \mathbb{L}^{\alpha} \mathcal{T}^{\alpha} \Psi_k \\ &= \max \langle \pi, R + \gamma P V_k \rangle + \alpha \mathcal{H}(\pi) \\ &\leq R_{\max} + \gamma \|V_k\|_{\infty} + \alpha \log |\mathcal{A}| \\ &\leq R_{\max} + \frac{\gamma}{1-\gamma} (3 \|V_0\|_{\infty} + R_{\max} + \alpha \log |\mathcal{A}|) + \alpha \log |\mathcal{A}| \\ &\leq \frac{\gamma}{1-\gamma} 3 \|V_0\|_{\infty} + \left(\frac{1-\gamma}{1-\gamma} + \frac{\gamma}{1-\gamma} \right) (R_{\max} + \alpha \log |\mathcal{A}|) \\ &\leq \frac{1}{1-\gamma} (3 \|V_0\|_{\infty} + R_{\max} + \alpha \log |\mathcal{A}|) \end{aligned}$$

Since (13) holds for $k = 0$ also from $1 \leq \frac{3}{1-\gamma}$, the claim follows. \blacksquare

Lemma 10. *Let $\|\Psi_0\|_{\infty} < \infty$ and \mathcal{T}' be an operator satisfying the conditions of Lemma 8. Then for all $k \in \mathbb{N}$,*

$$\Psi_k \leq \frac{1}{1-\gamma} (R_{\max} + \|\Psi_0\|_{\infty} + \gamma \alpha \log |\mathcal{A}|) \quad (18)$$

and

$$\Psi_k \geq -\frac{1}{(1-\beta)(1-\gamma)} \left((1+\beta) R_{\max} + (\gamma+\beta) (3 \|V_0\|_{\infty} + \alpha \log |\mathcal{A}|) \right) - \|\Psi_0\|_{\infty}.$$

Proof. Assume that, the inequality (18) holds up to $k \in \mathbb{N}$. Then, it holds that

$$\begin{aligned}
\Psi_k &= \mathcal{T}'\Psi_k \\
&\leq \mathcal{T}^\alpha\Psi_k \\
&= R + \gamma P\mathbb{L}^\alpha\Psi_k \\
&= R + \gamma P(\langle \pi_{k+1}, \Psi_k \rangle + \alpha\mathcal{H}(\pi_{k+1})) \\
&\leq R_{\max} + \gamma\|\Psi_k\|_\infty + \gamma\alpha \log|\mathcal{A}| \\
&\leq R_{\max} + \frac{\gamma}{1-\gamma}(R_{\max} + \|\Psi_0\|_\infty + \gamma\alpha \log|\mathcal{A}|) + \gamma\alpha \log|\mathcal{A}| \\
&= \left(\frac{1-\gamma}{1-\gamma} + \frac{\gamma}{1-\gamma}\right)(R_{\max} + \gamma\alpha \log|\mathcal{A}|) + \frac{\gamma}{1-\gamma}\|\Psi_0\|_\infty \\
&\leq \frac{1}{1-\gamma}(R_{\max} + \|\Psi_0\|_\infty + \gamma\alpha \log|\mathcal{A}|).
\end{aligned}$$

Since Ψ_0 satisfies (18) also from $1 \leq \frac{1}{1-\gamma}$, the upper bound (18) holds for all $k \in \mathbb{N}$. Now, we also have

$$\begin{aligned}
\Psi_{k+1} &= \mathcal{T}'\Psi_k \\
&\geq \mathcal{T}^\alpha\Psi_k - \beta(V_k - \Psi_k) \\
&= R + \gamma PV_k - \beta V_k + \beta\Psi_k \\
&\stackrel{(a)}{\geq} -R_{\max} - (\gamma + \beta)V_{\max}^{\text{SGI}} + \beta\Psi_k \\
&= -c_{\max} + \beta\Psi_k,
\end{aligned}$$

where (a) follows from Lemma 9 and $c_{\max} = R_{\max} + (\gamma + \beta)V_{\max}^{\text{SGI}} > 0$. Using the above recursively, we obtain

$$\begin{aligned}
\Psi_{k+1} &\geq -(1 + \beta + \beta^2 + \dots + \beta^k)c_{\max} + \beta^{k+1}\Psi_0 \\
&\geq -\frac{1}{1-\beta}c_{\max} - \|\Psi_0\|_\infty \\
&= -\frac{1}{1-\beta}\left(R_{\max} + \frac{\gamma + \beta}{1-\gamma}(R_{\max} + 3\|V_0\|_\infty + \alpha \log|\mathcal{A}|)\right) - \|\Psi_0\|_\infty \\
&= -\frac{1}{(1-\beta)(1-\gamma)}\left((1 + \beta)R_{\max} + (\gamma + \beta)(3\|V_0\|_\infty + \alpha \log|\mathcal{A}|)\right) - \|\Psi_0\|_\infty.
\end{aligned}$$

■

Theorem 4 (Theorem 1 in the main text). *Let $\Psi \in \mathbb{R}^{S \times \mathcal{A}}$, $V = \mathbb{L}^\alpha\Psi$, $\mathcal{T}^\alpha\Psi = R + \gamma P\mathbb{L}^\alpha\Psi$ and \mathcal{T}' be an operator with the properties that $\mathcal{T}'\Psi \leq \mathcal{T}^\alpha\Psi$ and $\mathcal{T}'\Psi \geq \mathcal{T}^\alpha\Psi - \beta(V - \Psi)$. Consider the sequence $\Psi_{k+1} := \mathcal{T}'\Psi_k$ with $\Psi_0 \in \mathbb{R}^{S \times \mathcal{A}}$, and let $V_k = \mathbb{L}^\alpha\Psi_k$. Further, with an abuse of notation, we write $V_\tau^* \in \mathbb{R}^S$ as the unique fixed point of the operator $\mathcal{T}^\tau V = \mathbb{L}^\tau(R + \gamma PV)$. Then, the sequence $(V_k)_{k \in \mathbb{N}}$ converges, and the limit $\tilde{V} = \lim_{k \rightarrow \infty} V_k$ satisfies $V_\tau^* \leq \tilde{V} \leq V_\alpha^*$. Furthermore, $\limsup_{k \rightarrow \infty} \Psi_k \leq Q_\alpha^*$ and $\liminf_{k \rightarrow \infty} \Psi_k \geq \frac{1}{1-\beta}(\tilde{Q} - \beta\tilde{V})$, where $\tilde{Q} = R + \gamma P\tilde{V}$.*

Proof. Upper Bound. From $\mathcal{T}'\Psi \leq \mathcal{T}^\alpha\Psi$ and observing that \mathcal{T}^α has a unique fixed point, we have

$$\limsup_{k \rightarrow \infty} \Psi_k = \limsup_{k \rightarrow \infty} (\mathcal{T}')^k \Psi_0 \leq \limsup_{k \rightarrow \infty} (\mathcal{T}^\alpha)^k \Psi_0 = Q_\alpha^*. \quad (19)$$

We know that $V_k = \mathbb{L}^\alpha\Psi_k$ converges to $\tilde{V} = \lim_{k \rightarrow \infty} \mathbb{L}^\alpha\Psi_k$ by Lemma 8. Since Lemma 10 assures that the sequence $(\Psi_k)_{k \in \mathbb{N}}$ is bounded, we have that $\limsup_{k \rightarrow \infty} \mathbb{L}^\alpha\Psi_k \leq \mathbb{L}^\alpha \limsup_{k \rightarrow \infty} \Psi_k$ from Lemma 6. Thus, it holds that

$$\tilde{V} = \lim_{k \rightarrow \infty} V_k = \limsup_{k \rightarrow \infty} V_k = \limsup_{k \rightarrow \infty} \mathbb{L}^\alpha\Psi_k \leq \mathbb{L}^\alpha \limsup_{k \rightarrow \infty} \Psi_k \leq \mathbb{L}^\alpha Q_\alpha^* = V_\alpha^*. \quad (20)$$

Lower Bound. Now, it holds that

$$\begin{aligned}\Psi_{k+1} &= \mathcal{T}'\Psi_k \\ &\geq \mathcal{T}^\alpha\Psi_k - \beta(V_k - \Psi_k) \\ &= R + \gamma PV_k - \beta V_k + \beta\Psi_k.\end{aligned}\tag{21}$$

From Lemma 9 and Lebesgue's dominated convergence theorem, we have

$$\lim_{k \rightarrow \infty} PV_k = P\tilde{V}.\tag{22}$$

Let $\bar{\Psi} := \liminf_{k \rightarrow \infty} \Psi_k$. Taking the liminf of both sides of (21) and from the fact $\liminf_{k \rightarrow \infty} V_k = \lim_{k \rightarrow \infty} V_k = \tilde{V}$ we obtain

$$\begin{aligned}\bar{\Psi} &\geq R + \gamma P\tilde{V} - \beta\tilde{V} + \beta\bar{\Psi} \\ &= \tilde{Q} - \beta\tilde{V} + \beta\bar{\Psi},\end{aligned}$$

where $\tilde{Q} = R + \gamma P\tilde{V}$. Thus it holds that

$$\bar{\Psi} \geq \frac{1}{1-\beta} (\tilde{Q} - \beta\tilde{V}).\tag{23}$$

Now, from Lemma 6 and 10, it holds that $\mathbb{L}^\alpha \liminf_{k \rightarrow \infty} \Psi_k \leq \liminf_{k \rightarrow \infty} \mathbb{L}^\alpha \Psi_k$. Thus, applying \mathbb{L}^α to the both sides of (23) and from Lemma 4 and 5, it follows that

$$\tilde{V} \geq \mathbb{L}^\tau \tilde{Q} = \mathbb{L}^\tau (R + \gamma P\tilde{V}) = \mathcal{T}^\tau \tilde{V}.$$

Using the above recursively, we have

$$\tilde{V} \geq \lim_{k \rightarrow \infty} (\mathcal{T}^\tau)^k \tilde{V} = V_\tau^*.\tag{24}$$

Combining (24) and (20), we have

$$V_\tau^* \leq \tilde{V} \leq V_\alpha^*.$$

■

B.4 PROOF OF PROPOSITION 1

We provide several lemmas that are used to prove Proposition 1.

Lemma 11. *The bounded gap-increasing operator satisfies $\mathcal{T}_{\pi_{k+1}}^{fg} \Psi_k \leq \mathcal{T}^\alpha \Psi_k$.*

Proof. From the non-positivity of A_k and the property of f and g , it holds that

$$\begin{aligned}\mathcal{T}_{\pi_{k+1}}^{fg} \Psi_k &= R + \beta f(A_k) + \gamma P \langle \pi_{k+1}, \Psi_k - g(A_k) \rangle \\ &\leq R + \gamma P \langle \pi_{k+1}, \Psi_k - g(A_k) \rangle \\ &\leq R + \gamma P \langle \pi_{k+1}, \Psi_k - A_k \rangle \\ &= R + \gamma P \mathbb{L}^\alpha \Psi_k \\ &= \mathcal{T}^\alpha \Psi_k.\end{aligned}$$

■

Lemma 12. *Consider the sequence $\Psi_{k+1} := \mathcal{T}_{\pi_{k+1}}^{fg} \Psi_k$ produced by the BAL operator (9) with $\Psi_0 \in \mathbb{R}^{S \times A}$, and let $V_k = \mathbb{L}^\alpha \Psi_k$. Then the sequence $(V_k)_{k \in \mathbb{N}}$ converges, if it holds that*

$$\lambda D_{\text{KL}}(\pi_{k+1} \| \pi_k) - \gamma P^{\pi_{k+1}} (\alpha \mathcal{H}(\pi_{k+1}) + \langle \pi_{k+1}, g(A_k) \rangle) \geq 0\tag{25}$$

for all $k \in \mathbb{N}$.

Proof. We follow similar steps as in the proof of Lemma 8. Let $\tilde{V} := \limsup_{k \rightarrow \infty} V_k$. It holds that

$$\begin{aligned}
V_{k+1} &= \mathbb{L}^\alpha \Psi_{k+1} = \langle \pi_{k+2}, \Psi_{k+1} \rangle + \alpha \mathcal{H}(\pi_{k+2}) \\
&\geq \langle \pi_{k+1}, \Psi_{k+1} \rangle + \alpha \mathcal{H}(\pi_{k+1}) \\
&= \left\langle \pi_{k+1}, \mathcal{T}_{\pi_{k+1}}^{fg} \Psi_k \right\rangle + \alpha \mathcal{H}(\pi_{k+1}) \\
&= \langle \pi_{k+1}, \mathcal{T}_{\pi_{k+1}} \Psi_k - \gamma P \langle \pi_{k+1}, g(A_k) \rangle + \beta f(A_k) \rangle + \alpha \mathcal{H}(\pi_{k+1}) \\
&\stackrel{(a)}{\geq} \langle \pi_{k+1}, \mathcal{T}_{\pi_{k+1}} \Psi_k - \gamma P \langle \pi_{k+1}, g(A_k) \rangle + \beta A_k \rangle + \alpha \mathcal{H}(\pi_{k+1}) \\
&\stackrel{(b)}{=} \langle \pi_{k+1}, \mathcal{T}_{\pi_{k+1}} \Psi_k \rangle + \tau \mathcal{H}(\pi_{k+1}) - \gamma \langle \pi_{k+1}, P \langle \pi_{k+1}, g(A_k) \rangle \rangle \\
&\stackrel{(c)}{=} \langle \pi_{k+1}, R + \gamma P (V_k - \alpha \mathcal{H}(\pi_{k+1})) \rangle + \tau \mathcal{H}(\pi_{k+1}) - \gamma P^{\pi_{k+1}} \langle \pi_{k+1}, g(A_k) \rangle \\
&\stackrel{(d)}{=} \langle \pi_{k+1}, Q_k + \gamma P (V_k - V_{k-1}) \rangle + \tau \mathcal{H}(\pi_{k+1}) - \gamma P^{\pi_{k+1}} (\alpha \mathcal{H}(\pi_{k+1}) + \langle \pi_{k+1}, g(A_k) \rangle) \\
&\stackrel{(e)}{=} V_k + \gamma P^{\pi_{k+1}} (V_k - V_{k-1}) + \lambda D_{\text{KL}}(\pi_{k+1} \| \pi_k) - \gamma P^{\pi_{k+1}} (\alpha \mathcal{H}(\pi_{k+1}) + \langle \pi_{k+1}, g(A_k) \rangle),
\end{aligned}$$

where (a) follows from the non-negativity of the advantage A_k and $x - f(x) \leq 0$, where (b) follows from $\langle \pi_{k+1}, A_k \rangle = \langle \pi_{k+1}, \alpha \log \pi_{k+1} \rangle = -\alpha \mathcal{H}(\pi_{k+1})$ and $(1-\beta)\alpha = \tau$, (c) follows from $V_k = \mathbb{L}^\alpha \Psi_k = \langle \pi_{k+1}, \Psi_k \rangle + \alpha \mathcal{H}(\pi_{k+1})$, (d) follows from $\mathcal{T}^\alpha \Psi_k = R + \gamma P \mathbb{L}^\alpha \Psi_k = R + \gamma P V_k = Q_{k+1}$, and (e) follows from $V_k = \mathbb{L}^\alpha \Psi_k = \langle \pi_{k+1}, Q_k \rangle + \tau \mathcal{H}(\pi_{k+1}) - \lambda D_{\text{KL}}(\pi_{k+1} \| \pi_k)$. Thus, if it holds that

$$\lambda D_{\text{KL}}(\pi_{k+1} \| \pi_k) - \gamma P^{\pi_{k+1}} (\alpha \mathcal{H}(\pi_{k+1}) + \langle \pi_{k+1}, g(A_k) \rangle) \geq 0$$

for all k , we have

$$V_{k+1} - V_k \geq \gamma P^{\pi_{k+1}} (V_k - V_{k-1}).$$

Therefore, by following the steps equivalent to the proof of Lemma 8, we have that $\liminf_{k \rightarrow \infty} V_k = \tilde{V}$ and V_k converges. \blacksquare

Lemma 13. *Let the conditions of Lemma 12 holds. Then for all $k \in \mathbb{N}$, the sequences $(V_k)_{k \in \mathbb{N}}$ and $(\Psi_k)_{k \in \mathbb{N}}$ are both bounded.*

Proof. Since the proof of Lemma 9 relies on the two inequalities $\mathcal{T}' \Psi \leq \mathcal{T}^\alpha \Psi$ and $V_{k+1} - V_k \geq \gamma P^{\pi_{k+1}} (V_k - V_{k-1})$, the boundedness of $(V_k)_{k \in \mathbb{N}}$ follows from the identical steps given Lemma 11 and Lemma 12. Furthermore, following the proof of Lemma 10, we can show that the sequence $(\Psi_k)_{k \in \mathbb{N}}$ is also bounded, where its lower bound has dependencies to c_f and c_g . \blacksquare

We are ready to prove Proposition 1. We also have an improved lower bound with an explicit dependency to c_f .

Proposition 2 (Proposition 1 in the main text). *1 Consider the sequence $\Psi_{k+1} := \mathcal{T}_{\pi_{k+1}}^{fg} \Psi_k$ produced by the BAL operator (9) with $\Psi_0 \in \mathbb{R}^{S \times A}$, and let $V_k = \mathbb{L}^\alpha \Psi_k$. Assume that for all $k \in \mathbb{N}$ it holds that*

$$\lambda D_{\text{KL}}(\pi_{k+1} \| \pi_k) - \gamma P^{\pi_{k+1}} (\alpha \mathcal{H}(\pi_{k+1}) + \langle \pi_{k+1}, g(A_k) \rangle) \geq 0. \quad (26)$$

Then, the sequence $(V_k)_{k \in \mathbb{N}}$ converges, and the limit $\tilde{V} = \lim_{k \rightarrow \infty} V_k$ satisfies $V_\alpha^ - \frac{1}{1-\gamma} (\beta c_f + \gamma \alpha \log |\mathcal{A}|) \leq \tilde{V} \leq V_\alpha^*$. Furthermore, $\limsup_{k \rightarrow \infty} \Psi_k \leq Q_\alpha^*$ and $\liminf_{k \rightarrow \infty} \Psi_k \geq \tilde{Q} - (\beta c_f + \gamma \alpha \log |\mathcal{A}|)$, where $\tilde{Q} = R + \gamma P \tilde{V}$.*

Proof. Upper Bound. Following the identical steps in the proof of Theorem 4, we obtain the upper bounds $\tilde{\Psi} := \limsup_{k \rightarrow \infty} \Psi_k \leq Q_\alpha^*$ and $\tilde{V} = \lim_{k \rightarrow \infty} V_k = \limsup_{k \rightarrow \infty} V_k \leq V_\alpha^*$ again from Lemma 11.

Lower Bound. It holds that

$$\begin{aligned}
\Psi_{k+1} &= \mathcal{T}_{\pi_{k+1}}^{fg} \Psi_k \\
&= \mathcal{T}_{\pi_{k+1}} \Psi_k - \gamma P \langle \pi_{k+1}, g(A_k) \rangle + \beta f(A_k) \\
&\stackrel{(a)}{\geq} \mathcal{T}_{\pi_{k+1}} \Psi_k - \beta c_f \\
&= R + \gamma P V_k - \beta c_f - \gamma \alpha P \mathcal{H}(\pi_{k+1}) \\
&\geq R + \gamma P V_k - \beta c_f - \gamma \alpha \log |\mathcal{A}|,
\end{aligned} \tag{27}$$

where (a) follows from the non-positivity of the soft advantage and the property of f and g . Following the proof of Lemma 10, we can show that the sequence $(\Psi_k)_{k \in \mathbb{N}}$ is bounded again, Now, V_k converges to \tilde{V} by Lemma 12. Furthermore, by Lemma 13 and Lebesgue's dominated convergence theorem, we have $\lim_{k \rightarrow \infty} P V_k = P \tilde{V}$. Let $\bar{\Psi} := \liminf_{k \rightarrow \infty} \Psi_k$. Taking the lim inf of both sides of (27), we obtain

$$\begin{aligned}
\bar{\Psi} &\geq R + \gamma P \tilde{V} - \beta c_f - \gamma \alpha \log |\mathcal{A}| \\
&= \tilde{Q} - (\beta c_f + \gamma \alpha \log |\mathcal{A}|),
\end{aligned}$$

where $\tilde{Q} = R + \gamma P \tilde{V}$. Now, from Lemma 6 and 10, it holds that $\mathbb{L}^\alpha \liminf_{k \rightarrow \infty} \Psi_k \leq \liminf_{k \rightarrow \infty} \mathbb{L}^\alpha \Psi_k$. Thus, applying \mathbb{L}^α to the both sides and from Lemma 4, we have

$$\tilde{V} \geq \mathbb{L}^\alpha \tilde{Q} - (\beta c_f + \gamma \alpha \log |\mathcal{A}|) = \mathcal{T}^\alpha \tilde{V} - (\beta c_f + \gamma \alpha \log |\mathcal{A}|).$$

Therefore, using this expression recursively we obtain

$$\tilde{V} \geq V_\alpha^* - \frac{1}{1-\gamma} (\beta c_f + \gamma \alpha \log |\mathcal{A}|).$$

■

B.5 PROOF OF THEOREM 2

Theorem 5 (Theorem 2 in the main text). *Let $(\pi_k)_{k \in \mathbb{N}}$ be a sequence of the policies obtained by BAL. Defining $\Delta_k^{fg} = \langle \pi^*, \beta (A_\tau^* - f(A_{k-1})) - \gamma P \langle \pi_k, A_{k-1} - g(A_{k-1}) \rangle \rangle$, it holds that:*

$$\|V_\tau^* - V_\tau^{\pi_{K+1}}\|_\infty \leq \frac{2\gamma}{1-\gamma} \left[2\gamma^{K-1} V_{\max}^\tau + \sum_{k=1}^{K-1} \gamma^{K-k-1} \|\Delta_k^{fg}\|_\infty \right]. \tag{28}$$

Proof. For the policy $\pi_{k+1} = \mathcal{G}^{0,\alpha}(\Psi_k)$, the operator $\mathcal{T}_{\pi_{k+1}}^{0,\tau}$ is a contraction map. Let $V_\tau^{\pi_{K+1}}$ denote the fixed point of $\mathcal{T}_{\pi_{K+1}}^{0,\tau}$, that is, $V_\tau^{\pi_{K+1}} = \mathcal{T}_{\pi_{K+1}}^{0,\tau} V_\tau^{\pi_{K+1}}$. Observing that $\pi_{k+1} = \mathcal{G}_{\pi_k}^{\lambda,\tau}(Q_k) = \mathcal{G}_{\pi_k}^{\lambda,\tau}(R + \gamma P V_{k-1})$, we have for $K \geq 1$,

$$\begin{aligned}
V_\tau^* - V_\tau^{\pi_{K+1}} &= \mathcal{T}_{\pi^*}^{0,\tau} V_\tau^* - \mathcal{T}_{\pi^*}^{0,\tau} V_{K-1} + \mathcal{T}_{\pi^*}^{0,\tau} V_{K-1} - \mathcal{T}^\tau V_{K-1} + \mathcal{T}^\tau V_{K-1} - \mathcal{T}_{\pi_{K+1}}^{0,\tau} V_\tau^{\pi_{K+1}} \\
&\stackrel{(a)}{\leq} \gamma P^{\pi^*} (V_\tau^* - V_{K-1}) + \gamma P^{\pi_{K+1}} (V_{K-1} - V_\tau^{\pi_{K+1}}) \\
&= \gamma P^{\pi^*} (V_\tau^* - V_{K-1}) + \gamma P^{\pi_{K+1}} (V_{K-1} - V_\tau^* + V_\tau^* - V_\tau^{\pi_{K+1}}) \\
&= (I - \gamma P^{\pi_{K+1}})^{-1} (\gamma P^{\pi^*} - \gamma P^{\pi_{K+1}}) (V_\tau^* - V_{K-1}),
\end{aligned} \tag{29}$$

where (a) follows from $\mathcal{T}_{\pi^*}^{0,\tau} V_{K-1} \leq \mathcal{T}^\tau V_{K-1} = \mathcal{T}_{\pi_{K+1}}^{0,\tau} V_{K-1}$ and the definition of $\mathcal{T}_{\pi^*}^{0,\tau}$.

We proceed to bound the term $V_\tau^* - V_{K-1}$:

$$\begin{aligned}
V_\tau^* - V_{K-1} &= \mathcal{T}_{\pi^*}^{0,\tau} V_\tau^* - \mathcal{T}_{\pi^*}^{0,\tau} V_{K-2} + \mathcal{T}_{\pi^*}^{0,\tau} V_{K-2} - \mathbb{L}^\alpha \Psi_{K-1} \\
&= \gamma P^{\pi^*} (V_\tau^* - V_{K-2}) + \Delta_{K-1},
\end{aligned}$$

where $\Delta_{K-1} = \mathcal{T}_{\pi^*}^{0,\tau} V_{K-2} - \mathbb{L}^\alpha \Psi_{K-1}$. Observing that

$$\begin{aligned}
\mathbb{L}^\alpha \Psi_{K-1} &= \langle \pi_K, \Psi_{K-1} \rangle + \alpha \mathcal{H}(\pi_K) \\
&= \max_{\pi} \langle \pi, \Psi_{K-1} \rangle + \alpha \mathcal{H}(\pi) \\
&\geq \langle \pi^*, \Psi_{K-1} \rangle + \alpha \mathcal{H}(\pi^*) \\
&= \langle \pi^*, R + \beta f(A_{K-2}) + \gamma P \langle \pi_{K-1}, \Psi_{K-2} - g(A_{K-2}) \rangle \rangle + (\tau + \beta \alpha) \mathcal{H}(\pi^*),
\end{aligned}$$

we have

$$\begin{aligned}
\Delta_{K-1} &= \langle \pi^*, R + \gamma P V_{K-2} \rangle + \tau \mathcal{H}(\pi^*) - \mathbb{L}^\alpha \Psi_{K-1} \\
&\leq \langle \pi^*, \gamma P V_{K-2} \rangle - \langle \pi^*, \beta f(A_{K-2}) + \gamma P \langle \pi_{k-1}, \Psi_{K-2} - g(A_{K-2}) \rangle \rangle - \beta \alpha \mathcal{H}(\pi^*) \\
&= \langle \pi^*, \beta (A_\tau^* - f(A_{K-2})) \rangle - \gamma P \langle \pi_{K-1}, A_{K-2} - g(A_{K-2}) \rangle \\
&=: \Delta_{K-1}^{fg}.
\end{aligned}$$

Thus, it follows that

$$\begin{aligned}
V_\tau^* - V_{K-1} &\leq \gamma P^{\pi^*} (V_\tau^* - V_{K-2}) + \Delta_{K-1}^{fg} \\
&\leq (\gamma P^{\pi^*})^{K-1} (V_\tau^* - V_0) + \sum_{k=1}^{K-1} (\gamma P^{\pi^*})^{K-k-1} \Delta_k^{fg}.
\end{aligned}$$

Plugging the above into (29) and taking $\|\cdot\|_\infty$ on both sides, we obtain

$$\|V_\tau^* - V_\tau^{\pi_{K+1}}\|_\infty \leq \frac{2\gamma}{1-\gamma} \left[2\gamma^{K-1} V_{\max}^\tau + \sum_{k=1}^{K-1} \gamma^{K-k-1} \|\Delta_k^{fg}\|_\infty \right]. \quad (30)$$

■

C ADDITIONAL EXPERIMENTAL DETAILS.

C.1 BAL ON GRID WORLD.

Figure 11 shows the grid world environment used in Section 5.1. The reward is $r = 1$ at the top-right and bottom left corners, $r = 2$ at the bottom-right corner and $r = 0$ otherwise. The action space is $\mathcal{A} = \{\text{North, South, West, East}\}$. An attempted action fails with probability 0.1 and random action is performed uniformly. We set $\gamma = 0.99$. We chose $\alpha = 0.02$ and $\beta = 0.99$, thus $\tau = (1 - \beta)\alpha = 0.0002$ and $\lambda = \beta\alpha = 0.0198$. Since the transition kernel P and the reward function R are directly available for this environment, we can perform the model-based M-VI (2) and BAL (10) schemes. We performed 100 independent runs with random initialization of Ψ by $\Psi_0(s, a) \sim \text{Unif}(-V_{\max}^\tau, V_{\max}^\tau)$. Figure 4 compares the normalized value of the suboptimality $\|V^{\pi_k} - V_\tau^*\|_\infty$, where we computed V_τ^* by the recursion $V_{k+1} = \mathcal{T}^\tau V_k = \mathbb{L}^\tau (R + \gamma P V_k)$ with $V_0(s) = 0$ for all state $s \in \mathcal{S}$.

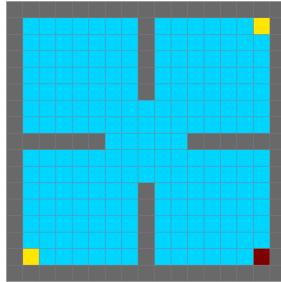


Figure 11: Grid world environment for model-based experiment.

C.2 MDAC ON MUJOCO AND DMC CONTROL SUITE.

We used PyTorch² and Gymnasium³ for all the experiments. We used reliable⁴ to calculate the IQM scores. MDAC is implemented based on SAC agent from CleanRL⁵. Each trial of

²<https://github.com/pytorch/pytorch>

³<https://github.com/Farama-Foundation/Gymnasium>

⁴<https://github.com/google-research/reliable>

⁵<https://github.com/vwxyzjn/cleanrl>

MDAC run was performed by a single NVIDIA V100 with 8 CPUs and took approximately 8 hours for 3M environment steps. For the baselines, we used SAC agent from CleanRL with default parameters from the original paper. We used author’s implementation⁶ for TD3 with default parameters.

Table 1 summarizes the hyperparameter values for MDAC, which are equivalent to the values for SAC except the additional β .

Table 1: MDAC Hyperparameters

Parameter	Value
optimizer	Adam (Kingma & Ba, 2015)
learning rate	$3 \cdot 10^{-4}$
discount factor γ	0.99
replay buffer size	10^6
number of hidden layers (all networks)	2
number of hidden units per layer	256
number of samples per minibatch	256
nonlinearity	ReLU
target smoothing coefficient by polyack averaging (κ)	0.005
target update interval	1
gradient steps per environmental step	1
reparameterized KL coefficient β	$1 - (1 - \gamma)^2$
entropy target $\bar{\mathcal{H}}$ to optimize $\tau = (1 - \beta)\alpha$	$-\dim(\mathcal{A})$

Per-environment results. Here, we provide per-environment results for ablation studies. Figure 13, 14, 15 and 16 show the per-environment results for Figure 5, 6, 8 and 9, respectively.

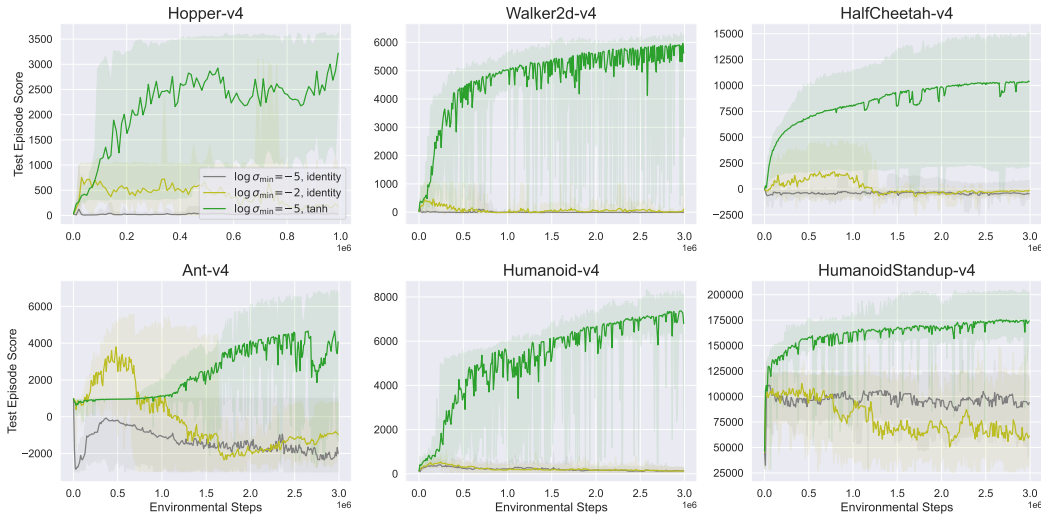


Figure 12: Per-environment performances for Figure 1. The mean scores of 10 independent runs are reported. The shaded region corresponds to the minimum and maximum scores over the 10 runs.

Quantities in TD target under clipping. Figure 17 compares the clipping frequencies for $f = g = \text{clip}(x, -1, 1)$ and $f = g = \text{clip}(x/10, -1, 1)$. Figure 18 compares the quantities in TD target.

⁶<https://github.com/sfujim/TD3>

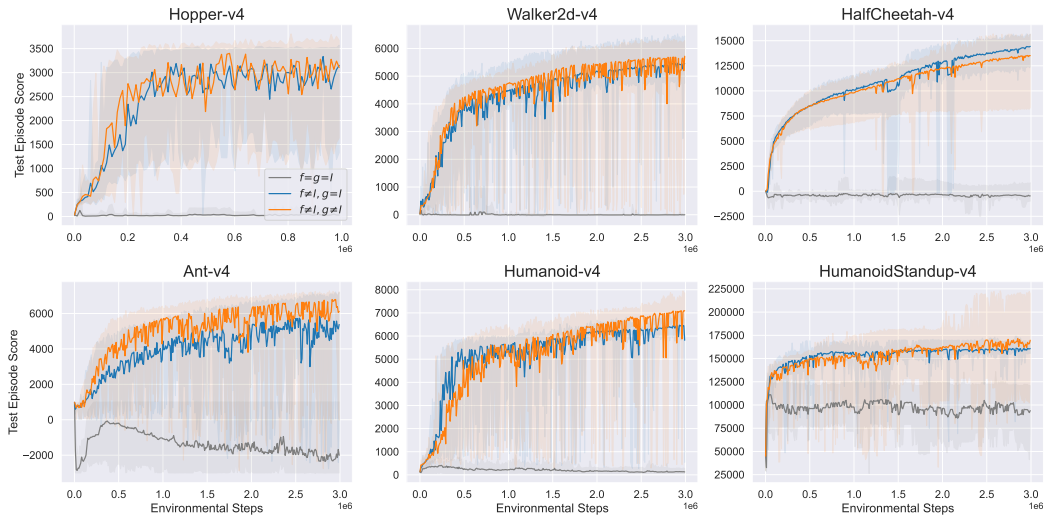


Figure 13: Per-environment performances for Figure 5. The mean scores of 10 independent runs are reported. The shaded region corresponds to the minimum and maximum scores over the 10 runs.

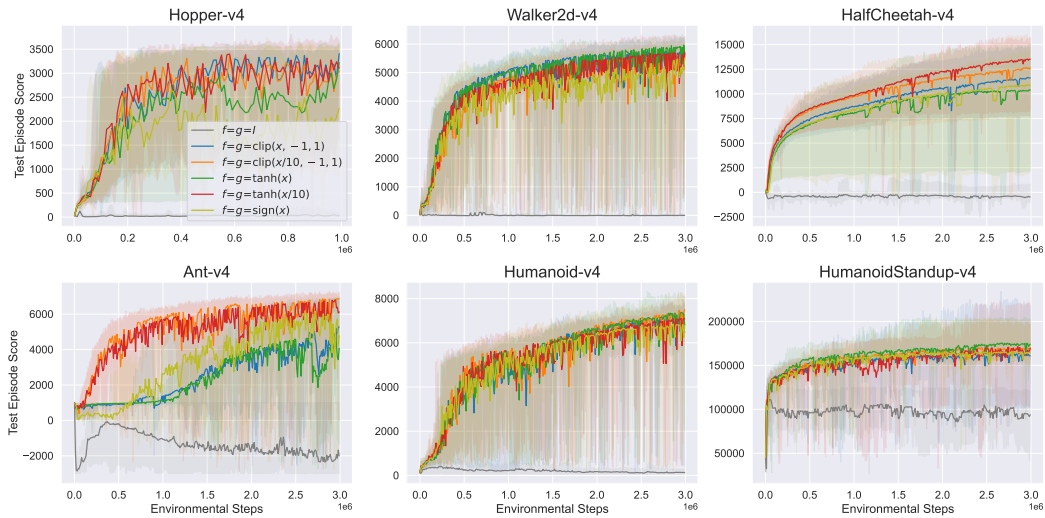


Figure 14: Per-environment performances for Figure 6. The mean scores of 10 independent runs are reported. The shaded region corresponds to the minimum and maximum scores over the 10 runs.

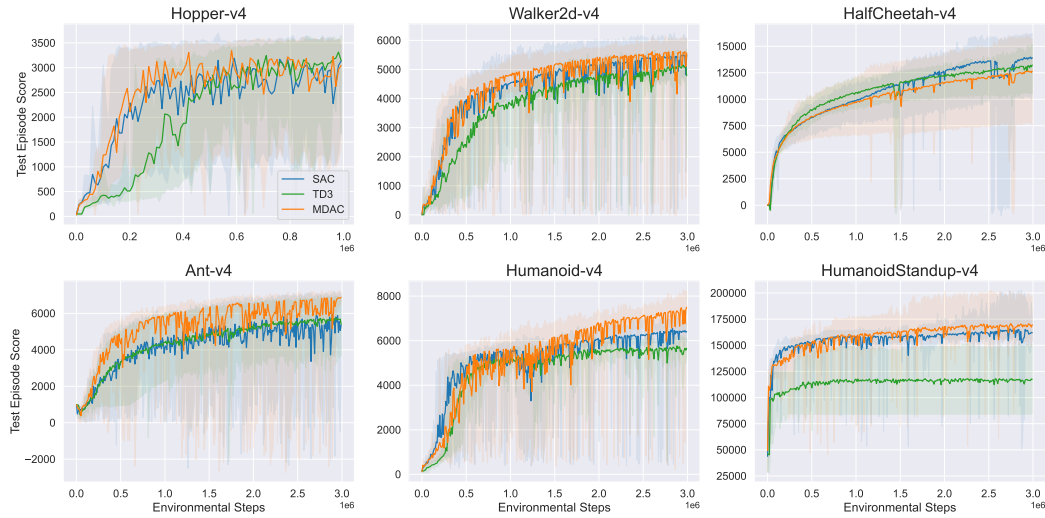


Figure 15: Per-environment performances. The mean scores of 10 independent runs are reported. The shaded region corresponds to the minimum and maximum scores over the 10 runs.

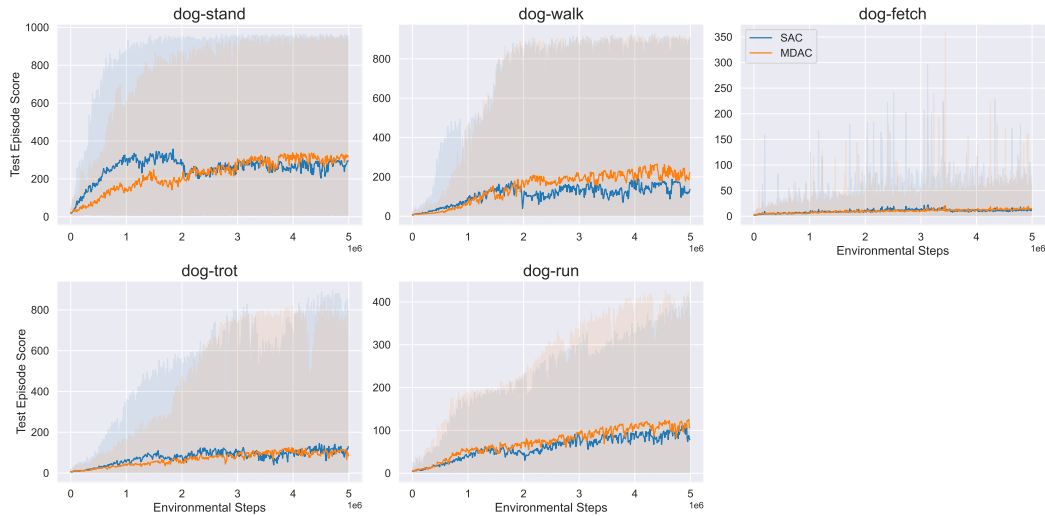


Figure 16: Per-environment performances in dog domain from DeepMind Control Suite. The mean scores of 30 independent runs are reported. The shaded region corresponds to the minimum and maximum scores over the 30 runs.

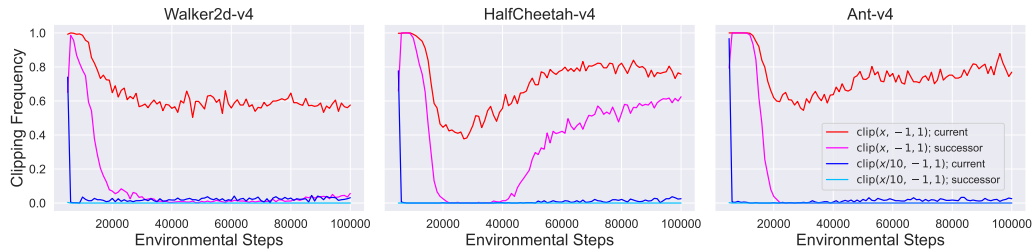


Figure 17: Comparison of clipping frequencies. Left: Walker2d-v4, Middle: HalfCheetah-v4. Right: Ant-v4.

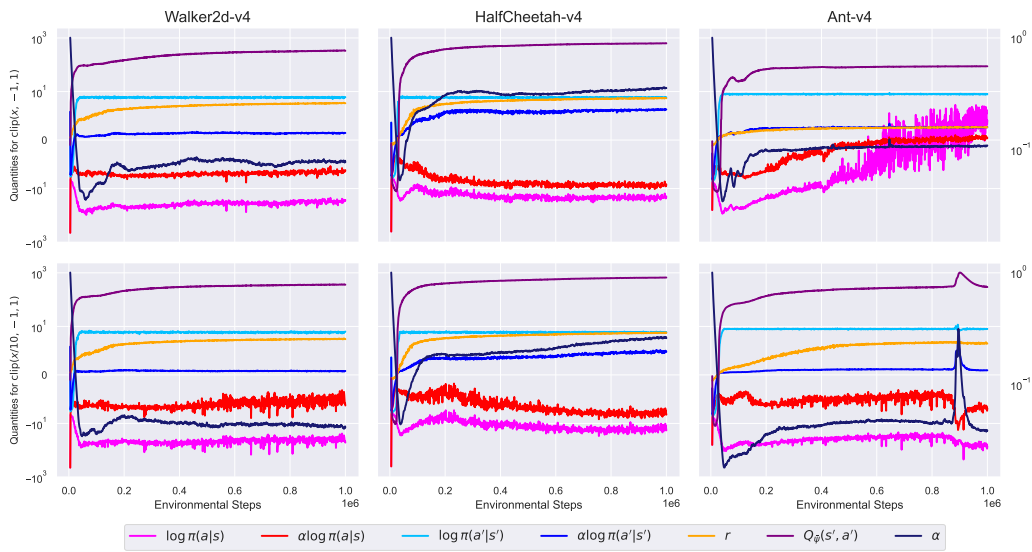


Figure 18: Scale comparison of the quantities in TD target. Top row: $\text{clip}(x, -1, 1)$, Bottom row: $\text{clip}(x/10, -1, 1)$, Left column: **Walker2d-v4**, Middle column: **HalfCheetah-v4**, Right column: **Ant-v4**.